Comparative Study of Voltage Source and Current Source Inverter Fed Induction Motor Drive

Mansour Oveissi

A Thesis

in

The Faculty

of

Engineering and Computer Science

Presented in Partial Fulfillment of the Requirements
for the degree of Master of Engineering
Concordia University
Montréal, Québec, Canada

December 1983

ABSTRACT

A COMPARATIVE STUDY OF VOLTAGE SOURCE AND CURRENT SOURCE INVERTER FED INDUCTION MOTOR DRIVE

Mansour Oveissi

A comparative analysis of a Squirrel-Cage Induction Motor fed from a Voltage Source inverter and Current Source inverter under steady-state is presented. The various losses, efficiency, steady-state torque, and pulsating torque parameters have been computed for both systems.

ACKNOWLEDGEMENTS

I gratefully acknowledge both Dr. J.F. Lindsay and Dr. K. Venkatesan who introduced me to AC drives. I am particularly indebted to Dr. Lindsay for his understanding, advice and supervision which helped me to accomplish this thesis. I wish also to thank Heather Rowe for her excellent typing and patience.

M. Oveissi

TABLE OF CONTENTS

LIST OF FIGURES

LIST OF TABLES

LIST OF PRINCIPAL SYMBOLS

SYMBOL	DESCRIPTION
L_d	DC LINK INDUCTANCE.
C_d	DC LINK CAPACITANCE.
I_d	DC LINK CURRENT.
V_d	DC LINK VOLTAGE.
V_{do}	NO LOAD DC LINK VOLTAGE.
V_{ml}	MAGNITUDE OF FUNDAMENTAL VOLTAGE.
I_{ml}	MAGNITUDE OF FUNDAMENTAL CURRENT.
W	ANGULAR SPEED.
θ	PHASE ANGLE.
I_{th}	THYRISTOR CURRENT.
V_{th}	THYRISTOR VOLTAGE.
V_c	SNUBBER CAPACITOR VOLTAGE.
V_{co}	INITIAL SNUBBER CAPACITOR VOLTAGE.
I_o	REVERSE RECOVERY CURRENT OF THYRISTOR.
F_1	FUNDAMENTAL FREQUENCY.
δ	ANGULAR DISPLACEMENT.
f	MAGNOMOTIVE FORCE.
ν	HARMONIC ORDER.
s	SLIP
I_m	MAGNETIZATION CURRENT.
E_1	FUNDAMENTAL AIRGAP VOLTAGE.
n	SYNCHRONOUS SPEED.

LIST OF PRINCIPAL SYMBOLS

SYMBOL	DESCRIPTION
N_1	ROTOR SPEED.
Z	IMPEDANCE.
I_{fL}	FULL LOAD CURRENT.
X_{pu}	PER UNIT INDUCTANCE.
θ_s	STANDSTILL.
I_s	STANDSTILL CURRENT.
m	NUMBER OF PHASES.
P	NUMBER OF POLES.
T	STEADY STATE TORQUE.
T_p	PULSATING TORQUE.
ϕ	FLUX.

CHAPTER I

INTRODUCTION

Industrial electric drives are defined as systems designed to process conversion of electrical energy into mechanical energy and to control the conversion process electrically. The basic components of an electric drive are electric motors, control systems, transmissional devices, and conversion equipment (inverter, rectifier and motor-generator equipment unit). Nowadays, the motor-generator equipment is replaced by static converters.

The electrical drive systems are segregated into direct current (DC), and alternating current (AC) drive systems. This classification is based on the type of electric motor being used. DC drives have been popular for many years in industry because of their attractive speed regulation. However, due to the large size of the DC motor, frequent maintenance requirements and the need to convert AC to DC power, its popularity has gradually decreased. These disadvantages have helped the AC drives to become more and more competitive with the DC drives. They have satisfied the applications where temporary shutdown is not afforded; in addition, the induction motor can be more readily installed in confined places.

The induction motor can also be directly connected to the mains in the case of power supply failure. In order for the induction motor to operate over the whole speed range and yet maintain a constant load torque by keeping the flux constant, the input voltage to frequency ratio (v/f) must remain constant (with voltage boost at low frequency). This condition is shown in the Speed-torque characteristic of Figure (1.1).

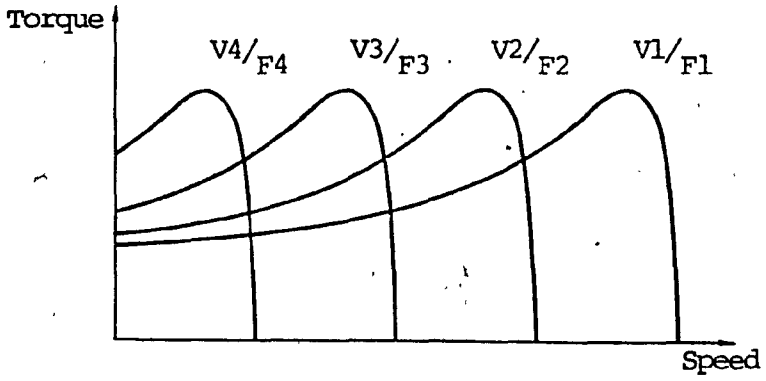

FIG. 1.1 SPEED-TORQUE CHARACTERISTIC OF INDUCTION MOTOR.

AC drives are mainly classified into direct and indirect converter drives. In direct converters (cycloconverters), the AC power is fed directly to the AC motor. The maximum output frequency of the cycloconverters is about one third of the supply frequency. For this reason, they have principally been used for applications in which motor size is large and the speed of operation is low. In indirect converters the AC power variation process is carried out in two stages. In the first stage the AC power, using either a diode or thyristor bridge rectifier, is rectified and then inverted to variable AC power by means of an inverter. This connection between converters is known as a DC link. This thesis concentrates solely on the DC link AC drive under the steady state condition. DC link AC converters are divided into voltage source inverter (VSI) and current source inverter (CSI). The VSI and the CSI are in fact duals of each other. The CSI supplies a controlled current to the motor whereas the VSI controls the voltage at the motor terminals. The voltage source, based on the method of its output control strategy, is classified as square-wave or pulse width modulated (PWM) variable frequency drive. The study of pulse width modulation is beyond the scope of this thesis; hence, attention will be given solely to the square wave type. A comparison is made with a CSI having the same output characteristic.

The square wave-forms contain a significant number of harmonics. When these harmonics are fed to an induction motor, they cause different

undesired effects which result in the derating of the motor. The additional harmonic losses, efficiency, harmonic torque and low speed torque pulsation are the quantities of interest in this thesis. The study is important due to the fact that the induction motor is the one which is the most used in industry. A comparative study of its performance when fed by VSI and CSI variable frequency power supply will help application engineers to select the most efficient system using a standard motor. If a specially customized design is more feasible, it will also be of help in the optimum design of the system. The increasing interest in exploring the potential of these two systems is attractive. A number of published papers point to the important role played by these systems in the overall economics of the country. Although many aspects of the two systems have been investigated, much more research is still required to fully comprehend them.

The circuit configuration representing the general basic power circuit of VSI and CSI as well as the gating sequence are described in detail by M. Abbas and Novotny [1]. They also show that VSI and CSI are duals of each other. This analysis was however, carried out solely for the ideal case. The efficiency and power factor of the square wave inverter drive have been studied by Skogsholm [13]. He was concerned with the general issue of power cost. He deals solely with the voltage source inverter. His method is based on measurement and it provides a good procedure for analysing the VSI systems. He also presents a classifications of losses

occuring in a rectifier-inverter drive. Among these losses are commutation and snubber losses. In order to account for these losses one must understand the basic principle of commutation and snubber circuits. Generalizing a specific formula to calculate losses in commutation circuits is difficult since they vary from one to another. However, they are all a function of power. A.J. Humphrey [3] analyses the commutation circuits and shows their importance in the cost of designing inverters. For snubber circuits, due to their basic general configuration, it is possible to devise some formulae to calculate their losses. Various aspects of the snubber circuit have been analysed in a number of papers. W. McMurray [4] presents an optimum design procedure for snubber circuits for semiconductors. P. Debruyne, H. Lawtseh [5], J.B. Rice, and L.E. Nickels [6] have extended McMurray's method by applying it to more practical cases. Barton [7] amalgamates the research of the above authors. His method of treatment is more suitable from an applications point of view.

The impact of VSI and CSI on the induction motor is discussed in great detail in a number of papers. Induction-motor losses due to nonsinusoidal supply wave forms have been studied by B.J. Chalmers and B.R. Sarikar[8]. They present an analytical and experimental study of losses. They also draw up a classification of losses. Methods for calculating these

losses have been studied elsewhere. The stray-load losses calculation is based on the method obtained by Alger[9]. Chalmers gives a method to calculate the iron losses in stator and rotor when both are due to skew leakage flux 8 . A comparative study of losses in the induction motor fed by a voltage and current source inverter is found in [10] . The different losses in induction motors fed by six-step current and voltage source inverters are calculated.

Low speed torque pulsation, a secondary consideration parameter produced by inverter drives in the induction motor, is studied by S.D.T. Robertson and K.M. Hebbar [11] . They describe the principle harmonic torques produced and conclude that the sixth harmonic is the most important one. They also provide an approximate expression to calculate torque pulsations.

The objective of this thesis is to bring together these main considerations by comparing the behaviour of VSI and CSI when fed to standard motors. The study will show the difference between these two systems and will provide data on performance which could be used by an application engineer. It will also help to improve customized motor design. In order to obtain an overall picture of efficiency, the losses of inverter and converter are included.

The text will be divided into three main chapters. Chapter II describes the basic principles involved in a DC link AC drive. The rectification and inversion process in both voltage and current source inverters are also considered. The classification of losses in the rectifier and in the inverter is included. Since some of these losses are contributed by the snubber and commutation circuits, a brief description of each is given. Chapter III studies the effect of nonsinusoidal wave forms on the induction motor performance and includes a comparison with the sinusoidal operation. The concept of time and space m.m.f. waves is developed. The calculation of current harmonic as well as harmonic torques is described. The effect of torque pulsation at low speed is presented and finally stability criteria under steady state are presented. Chapter IV investigates the differences in a typical induction motor performance when fed by VSI and CSI. Two programs for computing the effect of nonsinusoidal wave forms in an induction motor are described. Computation of the losses in the rectifier and inverter, the input power factor and the additional losses in the induction motor are given. The equivalent circuit used in calculating the losses is that of K. Venkatesan and J.F. Lindsay [10], where the contribution of higher harmonic is demonstrated.

The steady state torque, as well as the 6th, 12th and 18th harmonic torque pulsations are obtained and the efficiency is computed. Finally, the comparative tables demonstrate the differences between the two systems.

CHAPTER 2

THE RECTIFIER, DC LINK AND INVERTER

2.1 Introduction

This chapter is intended to provide a general description of the conversion unit which comprises of a rectifier, DC link, and inverter. This is probably the most common arrangement used to convert a constant frequency source into a variable frequency source suitable for a drive system. The AC source is first rectified and connected to the inverter by means of a DC link. The rectifier is normally a 3-phase bridge circuit. The DC link provides any filtering that is required and is the actual source for the inverter. The inverter is normally a thyristor bridge circuit although in smaller systems power transistors may find application. Because of the predominance of thyristor circuits, discussion will be limited to this form of inverter. The basic elements are shown in figure 2.1. To avoid confusion, the control and commutation circuitry are not shown.

In order to calculate the overall efficiency of an ac drive system, one must consider the losses contributed by each element of the system. Then all the losses must be added up to give the total loss.

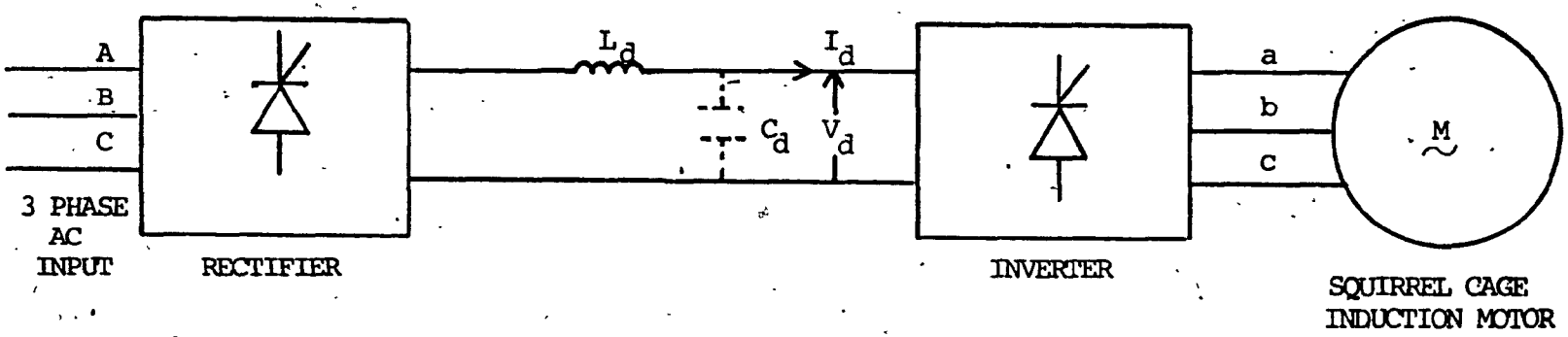

FIG. 2.1 SIMPLE BLOCK DIAGRAM OF A DC LINK CONVERTER.

Three phase bridge rectifier

The three phase bridge rectifier in a DC link AC drive is either a diode or a thyristor bridge type. The thyristor bridge is called a phase controlled rectifier since the output of the bridge can be controlled by varying the firing angle of the thyristor (α). On the other hand, a diode bridge has a fixed output. However, it could be considered a thyristor bridge by keeping the thyristor firing angle equal to zero. Under the α equal to zero condition, the principal of operation for both bridges is the same.

The rectifier

Since the operation of a diode bridge may be considered as a particular case of the operation of a thyristor bridge, only the latter will be explained.

Two cases of operation will be analysed. The first case corresponds to the firing angle α equal to 0. This case as was mentioned previously is the same for both thyristor and diode bridge. The second case corresponds to α being variable. This case is valid solely for the phase controlled thyristor bridge.

2.1.1 Firing Angle equal to zero

In this case, the delay angle α of the thyristors is zero and they behave as diodes. To study the sequence of operation, consider the bridge rectifier of fig. 2.2.

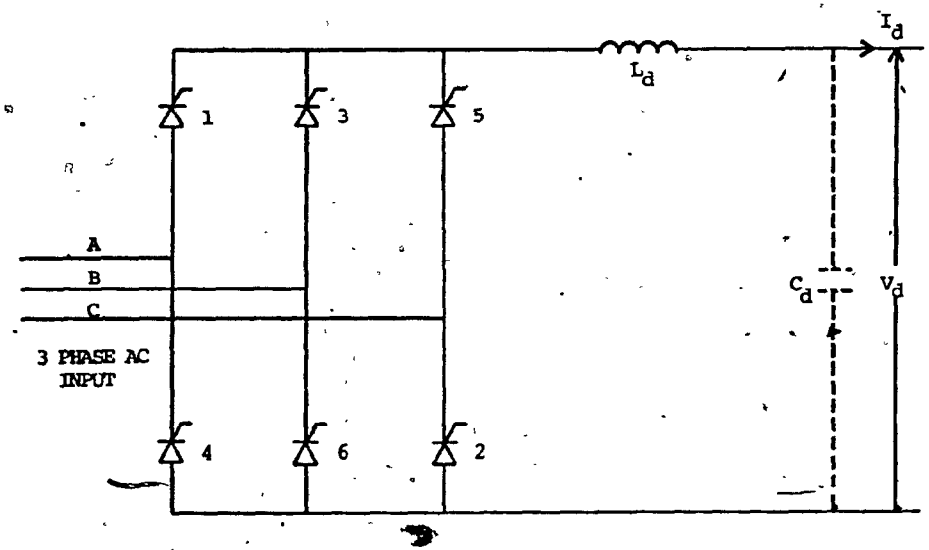

FIG. 2.2 THE BASIC THREE PHASE CONTROLLED BRIDGE RECTIFIER.

In most cases, the power supply is symmetrical, and the three phase voltages are displaced by 120° from each other, Fig. 2.3. Let us consider the rectifier at time t_1. At t_1, the phase B has the most positive value, and phase A has the most negative value. Therefore, thyristor 3, whose anode is more positive than the others, starts conducting. The current flows through thyristor three, through the load, and returns back to the source via thyristor 4 whose cathode is the most negative one.

At t_2, phases A and C are equal, thus creating the impression that two thyristors must conduct simultaneously. However, at t greater than t_2, phase C becomes the more positive one. Thyristor 3 turns off and thyristor 5 takes over the current. The current flows through thyristor five, through the load and then returns back to the source via thyristor 4 whose cathode has the most negative voltage. Thyristor 3 turned off automatically and current was transferred from thyristor 3 to thyristor 5. This commutation is therefore called natural commutation. The output voltage of the rectfier is shown in fig. 2.4, which is the algebriaic sum of the phase voltages.

The average output voltage is:

$$V_{do} = \frac{3\sqrt{6}}{\pi} V_{PH} = 2.34\ V_{PH} = 1.35\ V_L \qquad \ldots\ldots 2.1$$

where:

1) V_{do} is the average output voltage with zero delay and overlap angle.
2) V_{ph} is the r.m.s. phase voltage.
3) V_L is the r.m.s. line voltage.

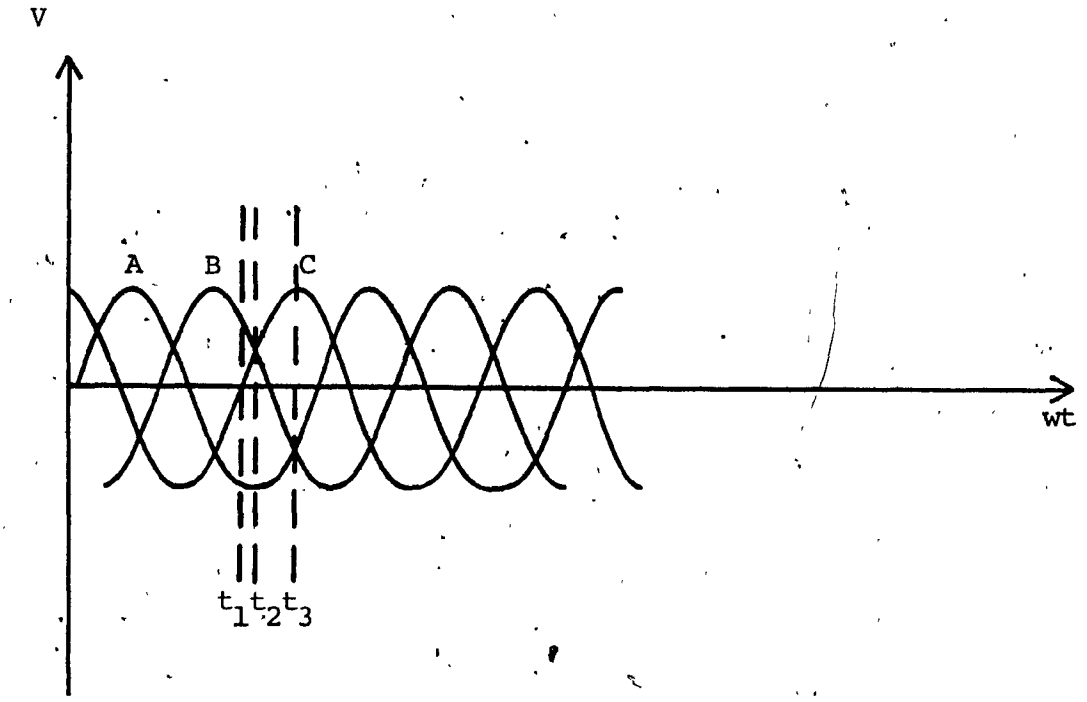

FIG. 2.3 3 PHASE AC SUPPLY VOLTAGE

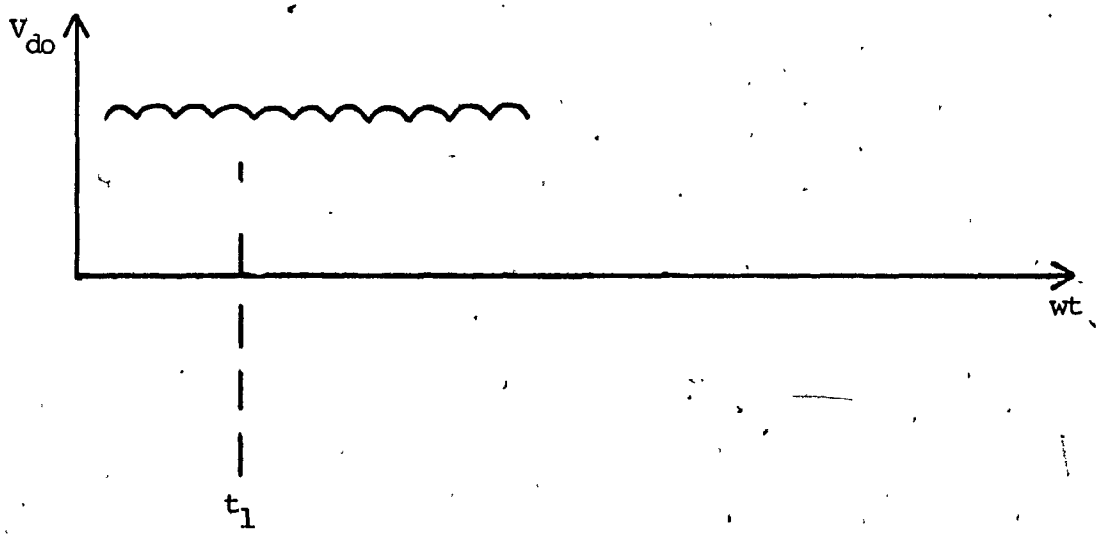

FIG. 2.4 RECTIFIER OUTPUT VOLTAGE

From fig. 2.4, each thyristor conducts for 120° in each cycle. Also, two thyristors conduct simultaneously in order to complete the circuit.

Current waveforms through each thyristor are illustrated in fig. 2.5. Assumption has been made that the load is very inductive.

2.1.2 Firing angle greater than zero

In this case, the average output voltage is varied by controlling the firing angle α . The angle α is measured from the point, commutation starts, Fig. 2.6. Because of this delay, the conducting thyristor conducts although its anode has not the most positive value.

The average voltage for $\alpha \leq 30^{\circ}$ is:

$$V_d = V_{do} \cos \alpha \qquad \ldots\ldots 2.2$$

for $\alpha \geq 30^{\circ}$

$$V_d = V_{do} \left\{ \frac{1 - \sin (\alpha - \frac{\pi}{m})}{2 \sin \frac{\pi}{m}} \right\} \qquad \ldots\ldots 2.3$$

Where m is number of phases.

[12].

Equations 2.2 and 2.3 are valid only for the Case of Continuous Current. Note that the voltage V_d across the load is the difference between V_{d1} and V_{d2}.

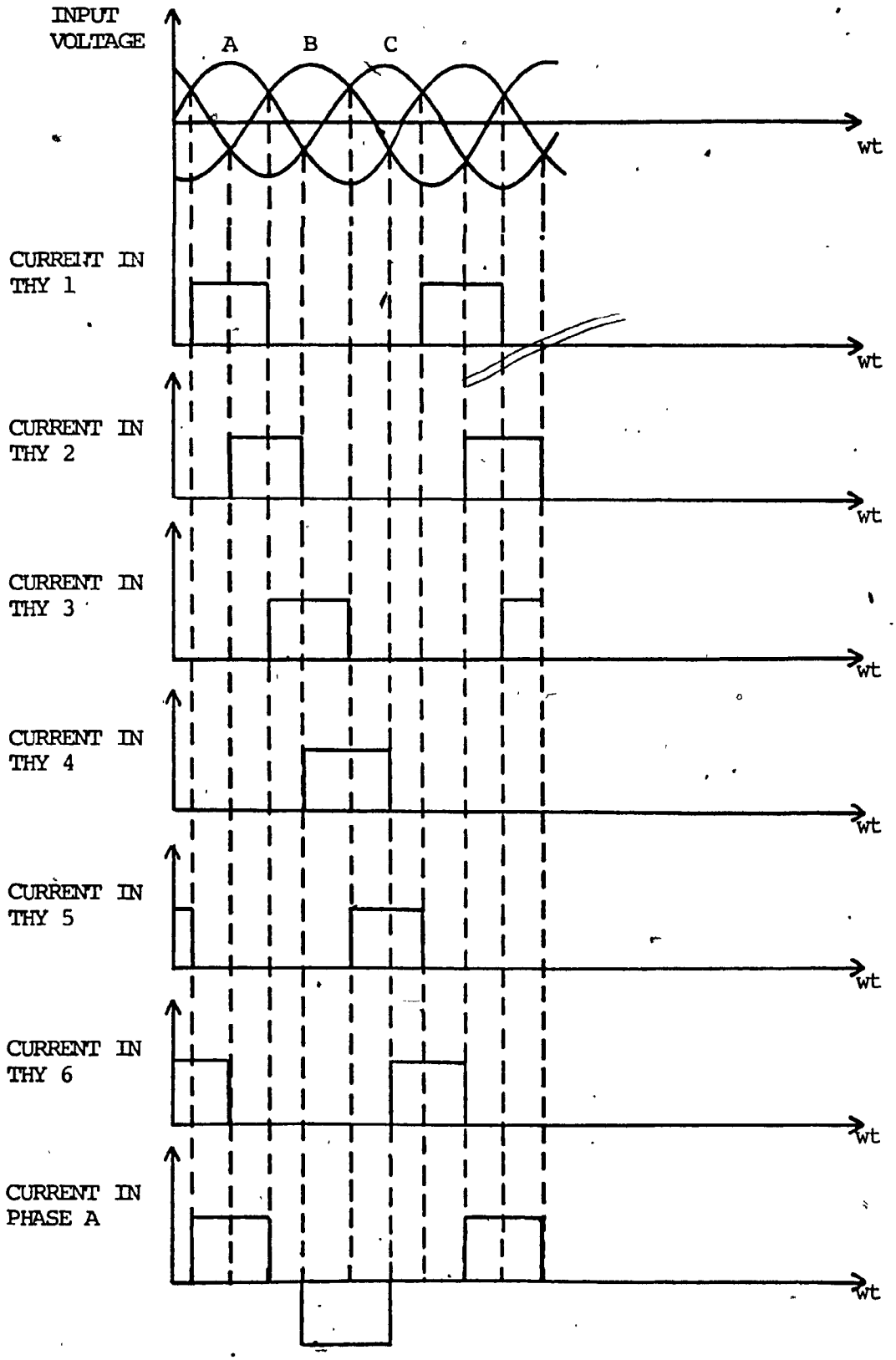

FIG. 2.5 THYRISTOR CURRENTS & PHASE A CURRENT FOR $\alpha = o$

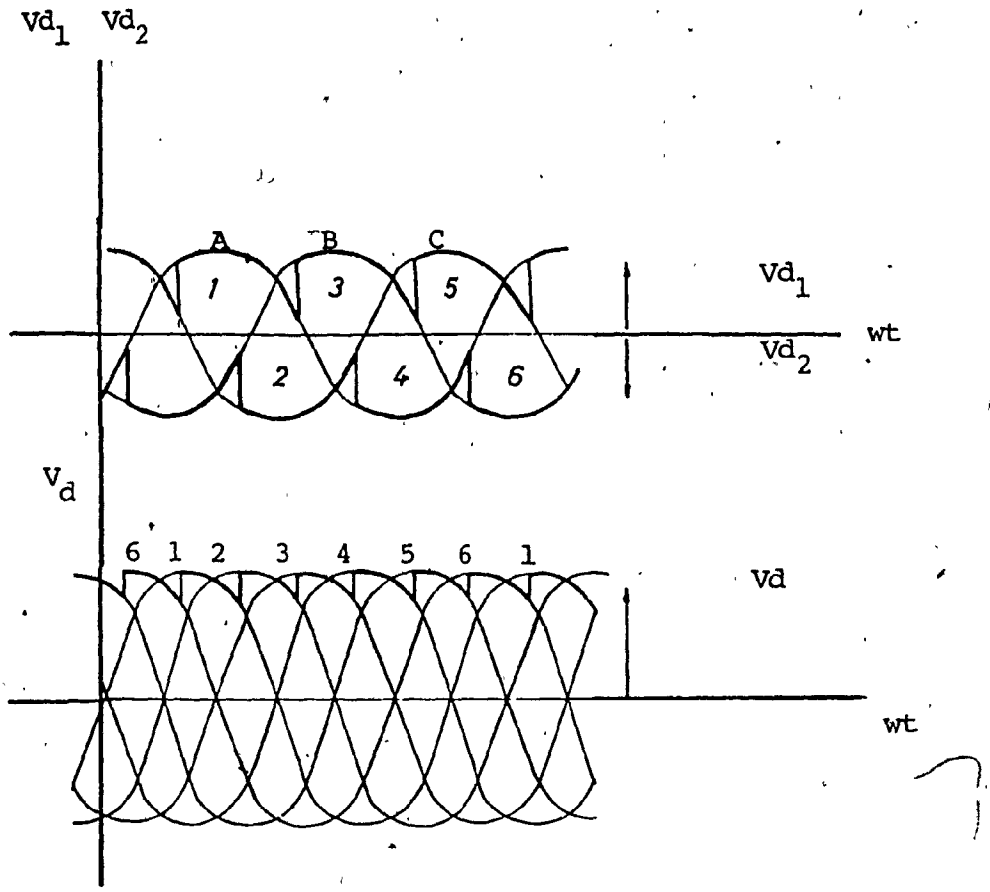

FIG. 2.6 THE OUTPUT VOLTAGE FOR α GREATER THAN ZERO.

$$V_d = V_{d1} - V_{d2}$$

The conduction sequence is shown in table 2.1.

CONDUCTION SEQUENCE	VD
1	A - B
2	A - C
3	B - C
4	B - A
5	C - A
6	C - B

Table (2.1) The conduction sequence of a 3-phase controlled rectifier.

2.2 DC Link and Inverter

AC drives having a DC link are classified according to the type of control placed on the inverter. A voltage source inverter (VSI) consists of a rectifier, an inductor, a capacitor bank which form a filter, and an inverter. Because of the capacitor bank, a VSI provides a constant voltage to the load, Fig. 2.7. A current source inverter (CSI) on the other hand, consists of a rectifier, an inductor and an inverter. Because of the inductor, a CSI provides constant torque to the load, Fig. 2.8.

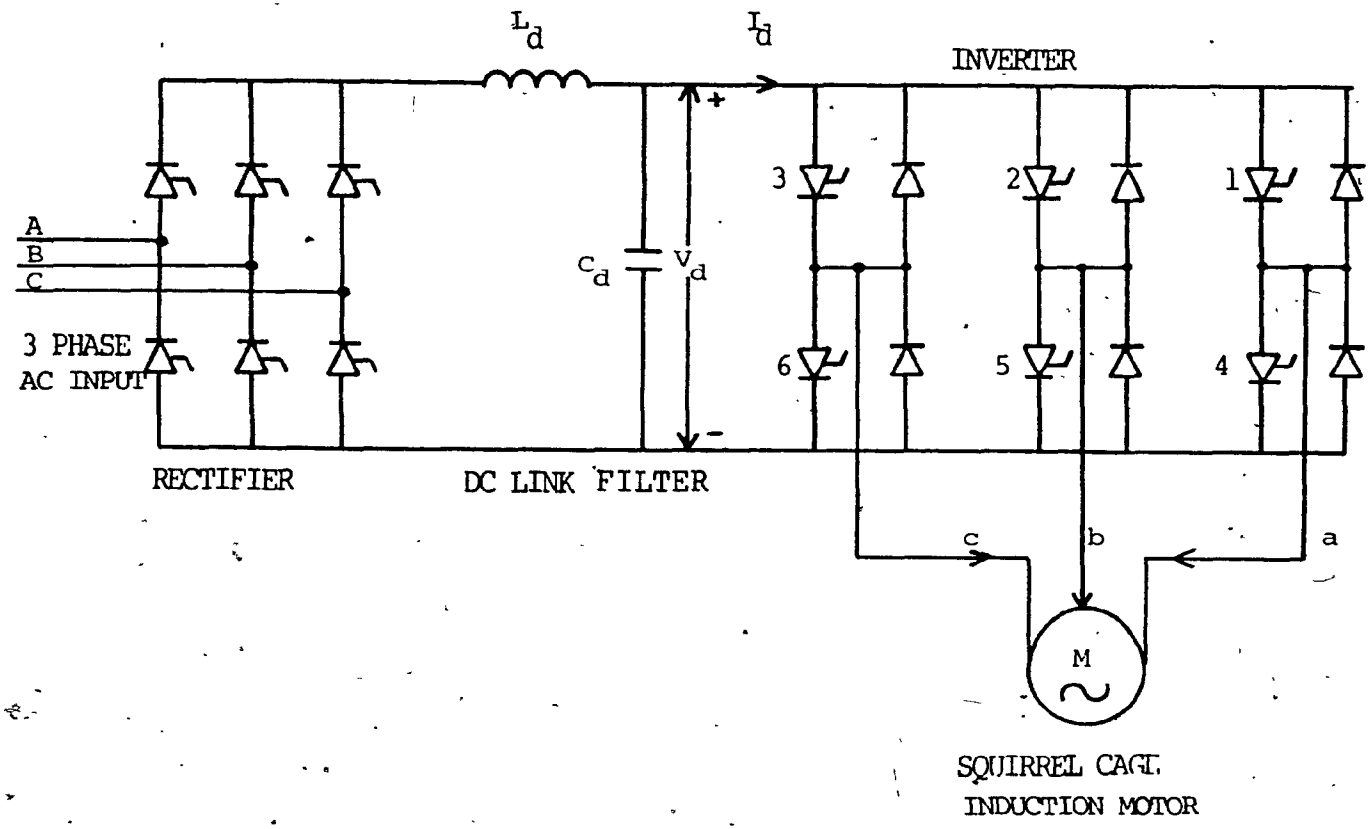

FIG. 2.7 SIX STEP VOLTAGE SOURCE INVERTER.

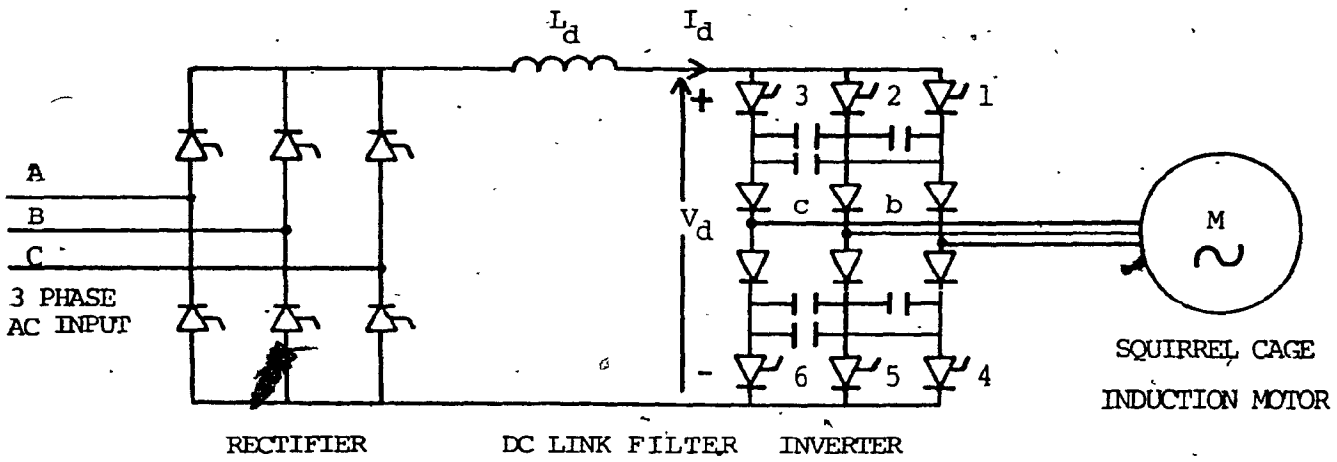

FIG. 2.8 SIX STEP, CURRENT SOURCE INVERTER.

2.2.1 Voltage Source Inverter

The two basic types of voltage source inverters are square wave and pulse width modulated (PWM). For the purpose of this thesis only the square wave type is explained. As stated previously, the VSI has a stiff output voltage. This is due to the large capacitance at its input.

The commutation must be forced. This is due to the lagging power factor produced by the induction motor.

In order to control the speed of the induction motor, a VSI has to provide variable frequency as well as variable voltage to the motor due to the fact that the synchronous speed of an induction motor is proportional to the input frequency. If the frequency is increased to increase the speed of the induction motor, without any increase in voltage, the air gap flux is reduced as a result of increased magnetizing reactance. The torque is therefore reduced.

This problem is usually overcome by changing both the frequency and the voltage, often with constant "volts per hertz". However, in the case of field-oriented control, it is possible to increase the frequency thus reducing the flux in a manner somewhat analogous to field weakening in a DC drive system.

Conduction Modes

The Conduction strategy of a VSI is such that three thyristors conduct simultaneously. But each thyristor is on for 180° over the whole period. To follow the modes of operation, consider the mode in which thyristors one, six, and five are conducting, Fig. 2.7. This mode lasts for 60°, and it happens when phase b is short circuited to phase c, Table 2.3. The current flows from the positive terminal, through the short circuit, and returns back to the source. The second mode starts 60° later, when thyristor six turns off, and thyristor three turns on. This mode like the preceding one lasts for 60° and it happens when phase c and a are short circuited together, Table 2.3. The current flow from the positive terminal, through the short circuit and finally returns back to the source. This procedure continues until all six modes have been carried out, Table 2.2.

Mode of Conduction	Conducting Thyristor	Duration of Conduction
1	1,5,6	60°
2	1,3,5	60°
3	3,5,4	60°
4	3,2,4	60°
5	4,2,6	60°
6	1,2,6	60°

Table 2.2 Modes of operation numerically.

Table 2.2 shows that each thyristor conducts for 180°, and every three thyristors conduct simultaneously. Table 2.3 represents Table 2.2 schematically.

1	2	3	4	5	6
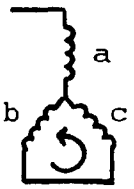	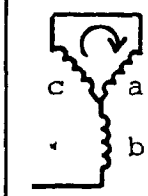	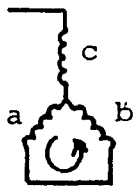	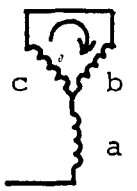	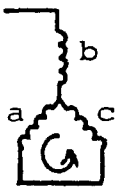	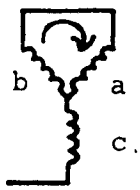

TABLE 2.3 Modes of operation schematically

Voltage Wave Forms

Fig. 2.9 illustrates the thyristor voltage wave forms as well as phase and line to line output voltage wave forms.

Current Wave Forms

Fig. 2.10 illustrates the current wave form corresponding to the voltage wave form V_{ab}. Note that the current wave form is growing and decaying exponentially. This is due to step changes in the voltages. It should also be noted that the load connection is Y.

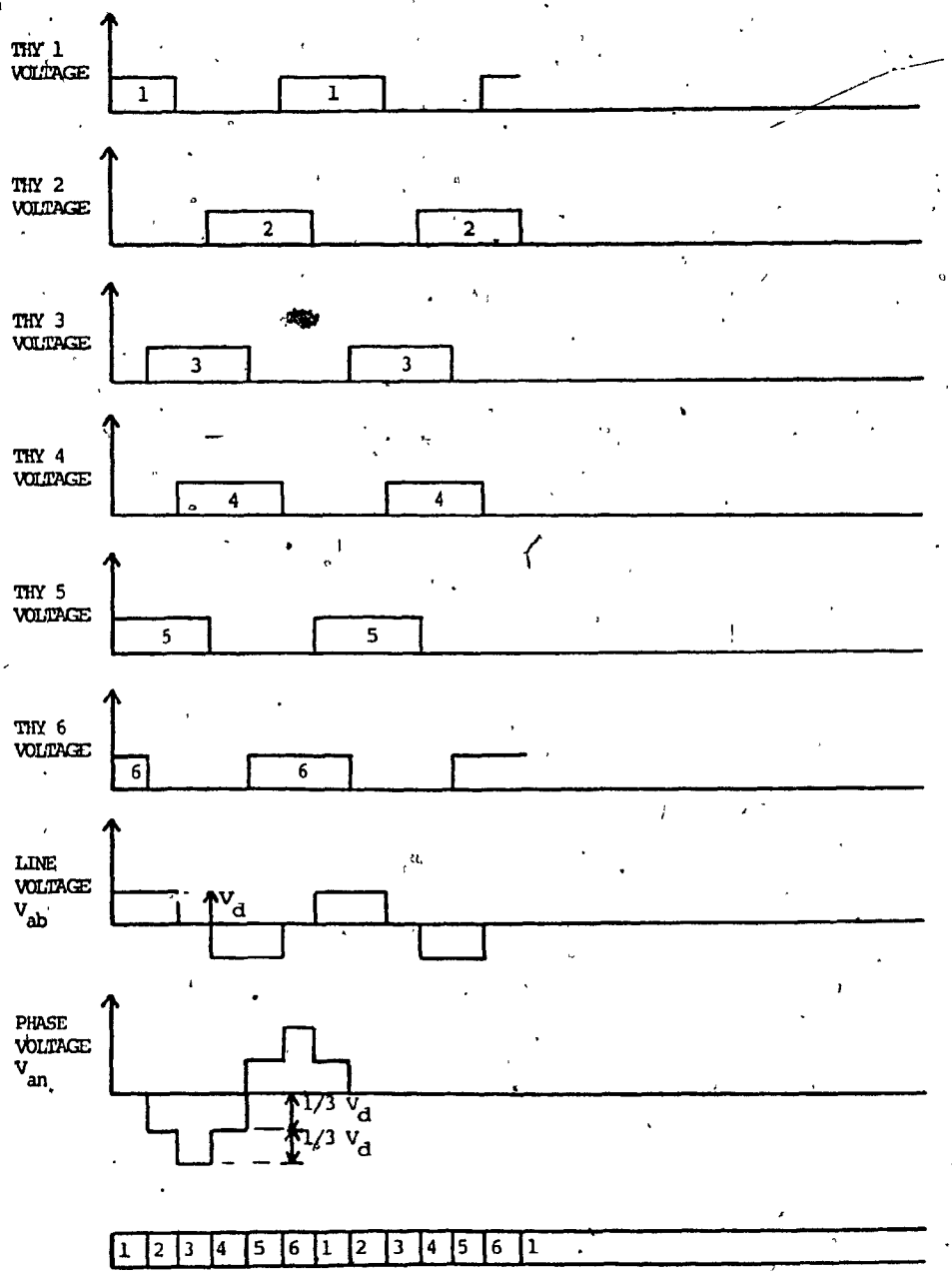

FIG. 2.9 THYRISTOR 1-6 VOLTAGES AND LINE TO LINE V_{ab} AND PHASE VOLTAGE V_{an}

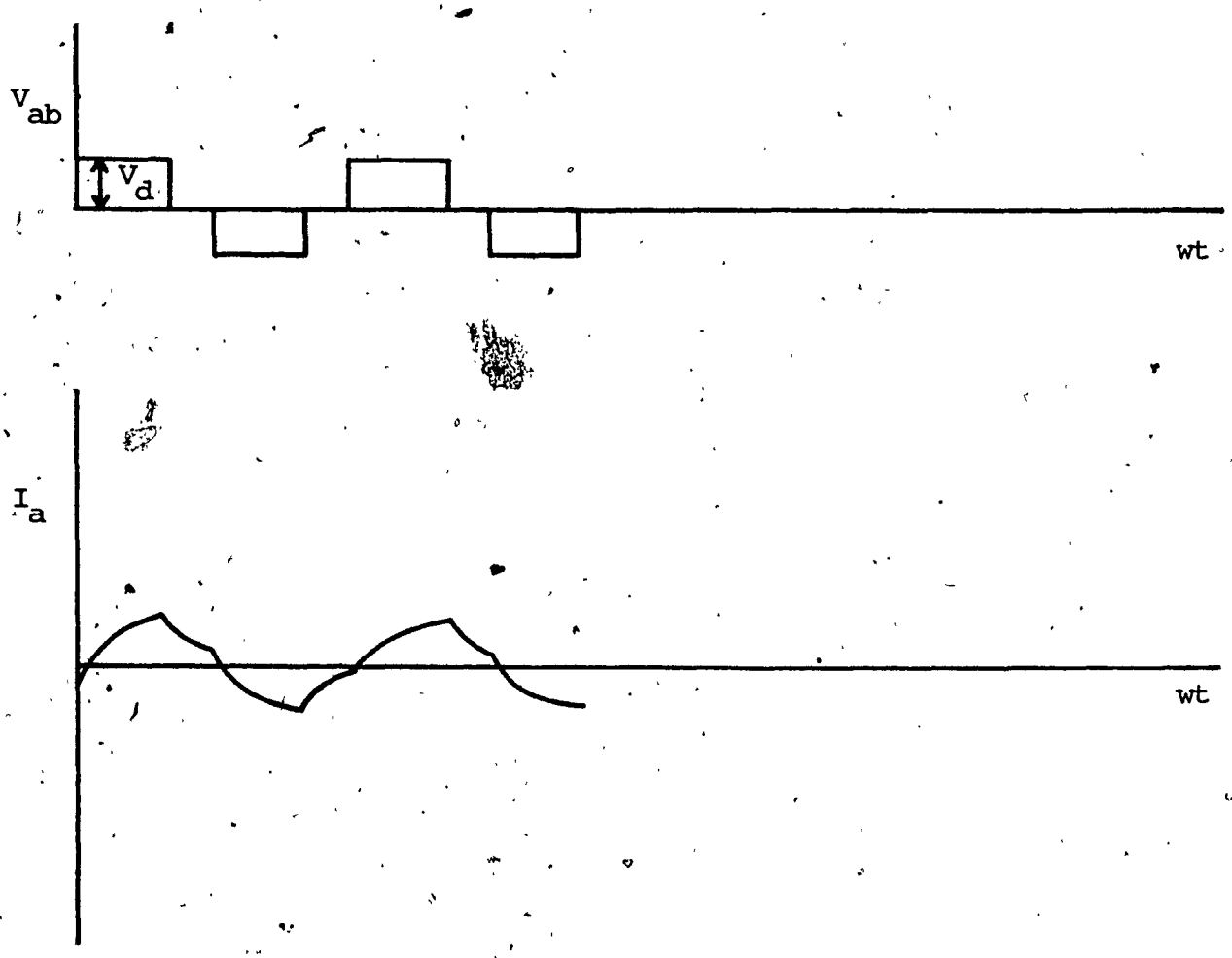

FIG. 2.10 CURRENT I_a CORRESPONDING TO V_{ab}.

Mathematical expression

From figure 2.9, it is evident that the output voltage wave forms are periodic and nonsinusoidal. Therefore a Fourier Series expansion is used to represent them mathematically [10].

Phase voltages:

$$V_a = V_{m1}\left[\sin\ wt - 1/5 \sin 5\ wt + 1/7\ \sin 7\ wt - 1/11 \sin 11\ wt + \ldots\right] \quad \ldots\ldots 2.4$$

$$V_b = V_{m1}\left[\sin\ (wt - \frac{2}{3}\pi) - 1/5 \sin\ (5wt + \frac{2}{3}\pi) - 1/7 \sin\ (7\ wt - \frac{2}{3}\pi)\right.$$
$$\left. - 1/11 \sin\ (11\ wt + \frac{2}{3}\pi) + \ldots\right] \quad \ldots\ldots 2.5$$

$$V_c = V_{m1}\left[\sin\ (wt + \frac{2}{3}\pi) - 1/5 \sin\ (5\ wt - \frac{2}{3}\pi) - 1/7 \sin\ (7\ wt + \frac{2}{3}\pi)\right.$$
$$\left. - 1/11 \sin\ (11\ wt - \frac{2}{3}\pi) + \ldots\right] \quad \ldots\ldots 2.6$$

PHASE CURRENTS:

$$I_a = I_1 \sin\ (wt - \theta_1) - I_5 \sin\ (5\ wt - \theta_5) +$$
$$I_7 \sin\ (wt - \theta_7) - I_{11} \sin\ (11\ wt - \theta_{11}) + \ldots \quad \ldots\ldots 2.7$$

$$I_b = I_1 \sin\ (wt - \frac{2}{3}\pi - \theta_1) - I_5 \sin\ (5\ wt + \frac{2}{3}\pi - \theta_5)$$
$$+ I_7 \sin\ (wt - \frac{2}{3}\pi - \theta_7) - I_{11} \sin\ (11\ wt + \frac{2}{3}\pi - \theta_{11}) + \ldots$$
$$\ldots\ldots 2.8$$

$$I_c = I_1 \text{ Sin } (wt - \frac{2}{3}\pi + \theta_1) - I_5 \text{ Sin } (5\,wt - \frac{2}{3}\pi - \theta_5)$$

$$+ I_7 \text{ Sin } (wt + \frac{2}{3}\pi - \theta_7) - I_{11} \text{ Sin } (11\,wt - \frac{2}{3}\pi - \theta_{11}) + \ldots$$

. . . . . 2.9

Where:

$$V_{ml} = \frac{2\sqrt{3}}{\pi} V_d$$

2.2.2 Current Source Inverter

A Current Source Inverter (CSI), is in fact the dual of the voltage source inverter. It consists of a rectifier, DC link (inductor), and a relatively simple inverter. The CSI has a stiff DC current at its input source. These inverters have received considerable interest in applications which require control over the torque.

The commutation is forced, just as in the VSI, but is less complex in circuitry. The need for forced commutation is due to the lagging power factor of the induction motor. There are many different methods of commutation design, including the Auto-Sequentially Commutated Inverter (ASCI) which is the most popular one, Fig.2.11, ASCI consists of six capacitors and six diodes. Each diode helps to store energy in the capacitors and isolate them from the load. In order to explain the commutation process, let us consider Thyristor 1 has been conducting, and is ready to be turned off. At this instant, thyristor three takes over the current. Thyristor 1 receives a negative voltage across its terminal from the capacitor and turns off. The situation prior to the commutation instant is illustrated in Fig. 2.12. The DC link current (Id) flows through thyristor 1, diode 1, phase A, phase B, diode 5, thyristor 5, and eventually returns back to the supply. At the commutation instant, a reverse capacitor voltage occurs across thyristor 1 forcing it to stop conduction. Thyristor 3 is turned on and takes over the current. This situation is shown in Fig. 2.13. I_d flows through thyristor 3, capacitor C3, diode D1, phase A, phase B, diode D5, thyristor 5 and returns back to the source. This process cont-

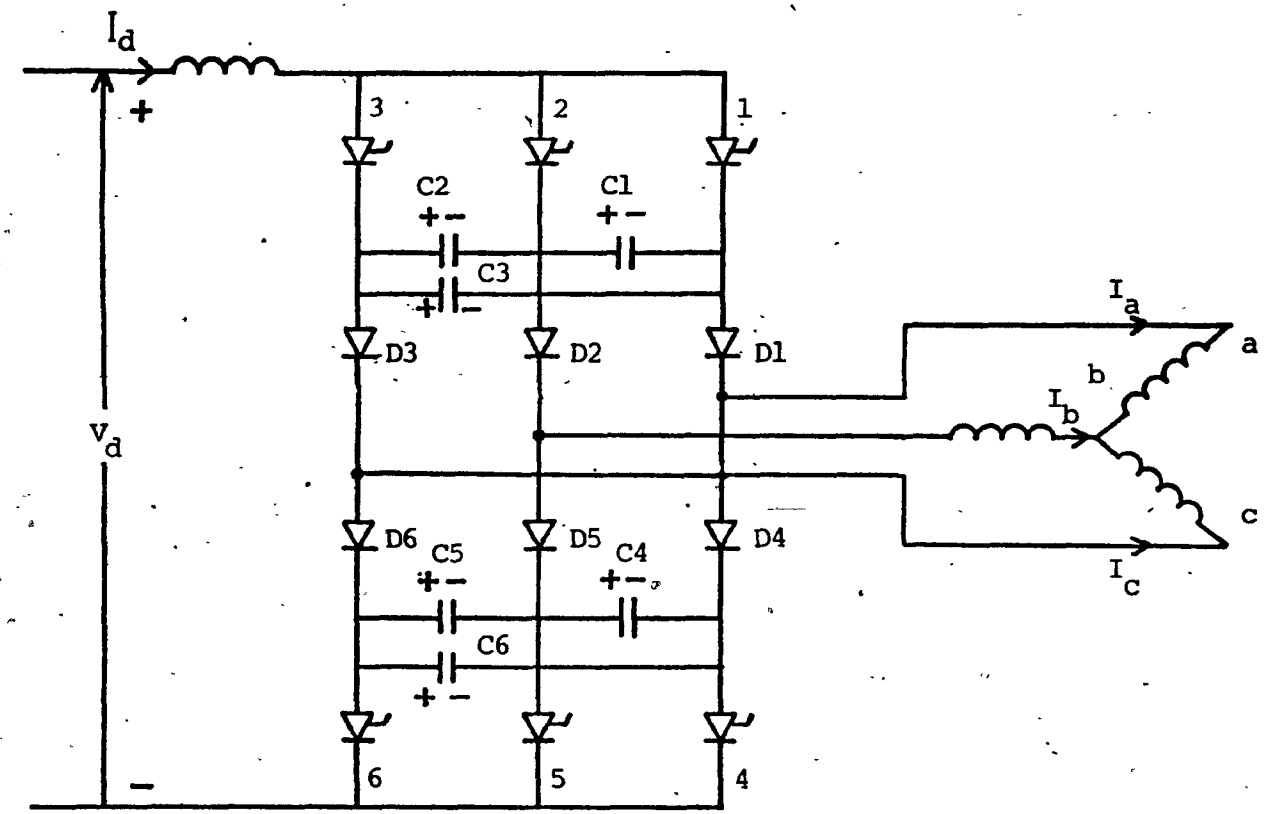

FIG. 2.11 CURRENT SOURCE INVERTER (CSI).

inues until the capacitor polarity reverses and forces diode 3 to conduct as shown in Fig. 2.14. This scheme terminates when the current through diode D1 and phase A reduces to zero. Thyristor 3 takes over I_d completely and completes the final stage of commutation, fig. 2.15.

It must be noted that every two thyristors conduct at the same time and each thyristor conducts for 120°. This is different from VSI. Table 2.4 and 2.5 illustrate the sequence of conduction numerically and schematically respectively.

SEQUENCE OF CONDUCTION	CONDUCTING THYRISTORS
1	1,5
2	3,5
3	3,4
4	2,4
5	2,4
6	1,6

Table 2.4 Sequence of Conduction of CSI numerically.

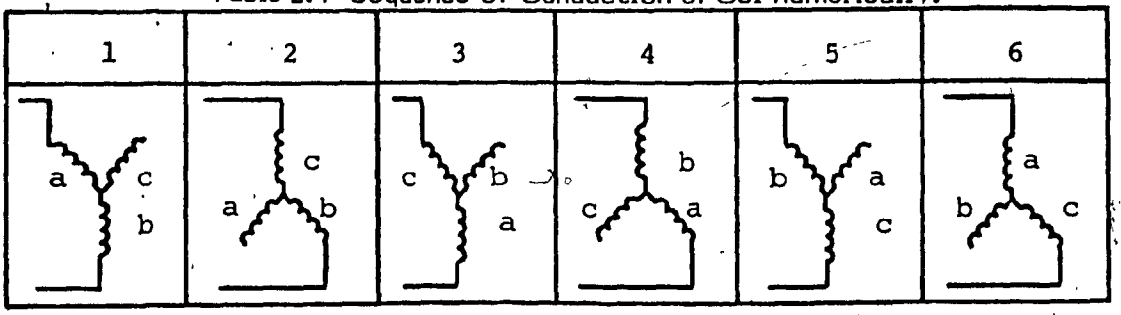

TABLE 2.5 · Sequence of Conduction of CSI schematically.

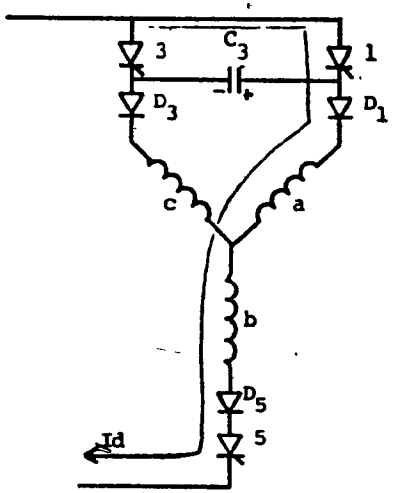

FIG. 2.12 THYRISTOR ONE IS CONDUCTING.

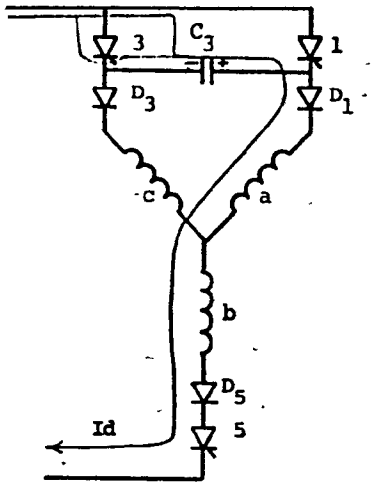

FIG. 2.13 INSTANT AFTER THE COMMUTATION.

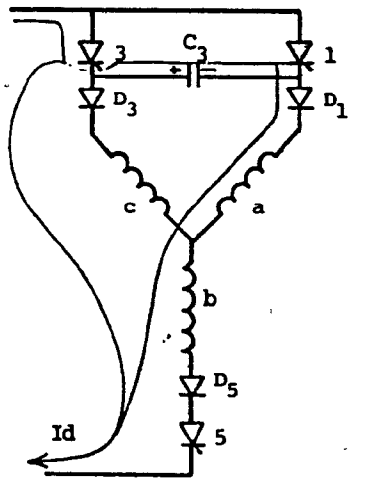

FIG. 2.14 THE I_d IS SPLITTED INTO TWO BRANCHES.

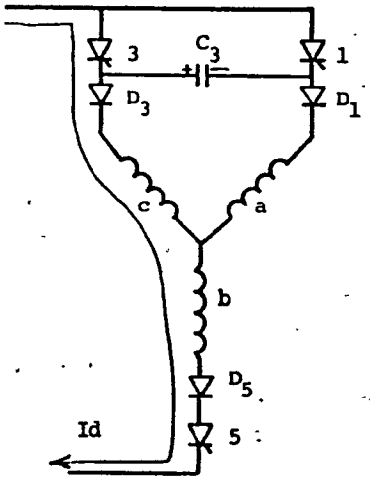

FIG. 2.15 THE COMMUTATION IS COMPLETE.

Waveforms

Thyristors current waveforms are shown in figure 2.16. Current wave forms corrsponding to phase B and C are the same as the current wave form of phase A, apart from the fact that they are displaced from each other by 120° in time. The phase voltage is shown in figure 2.17.

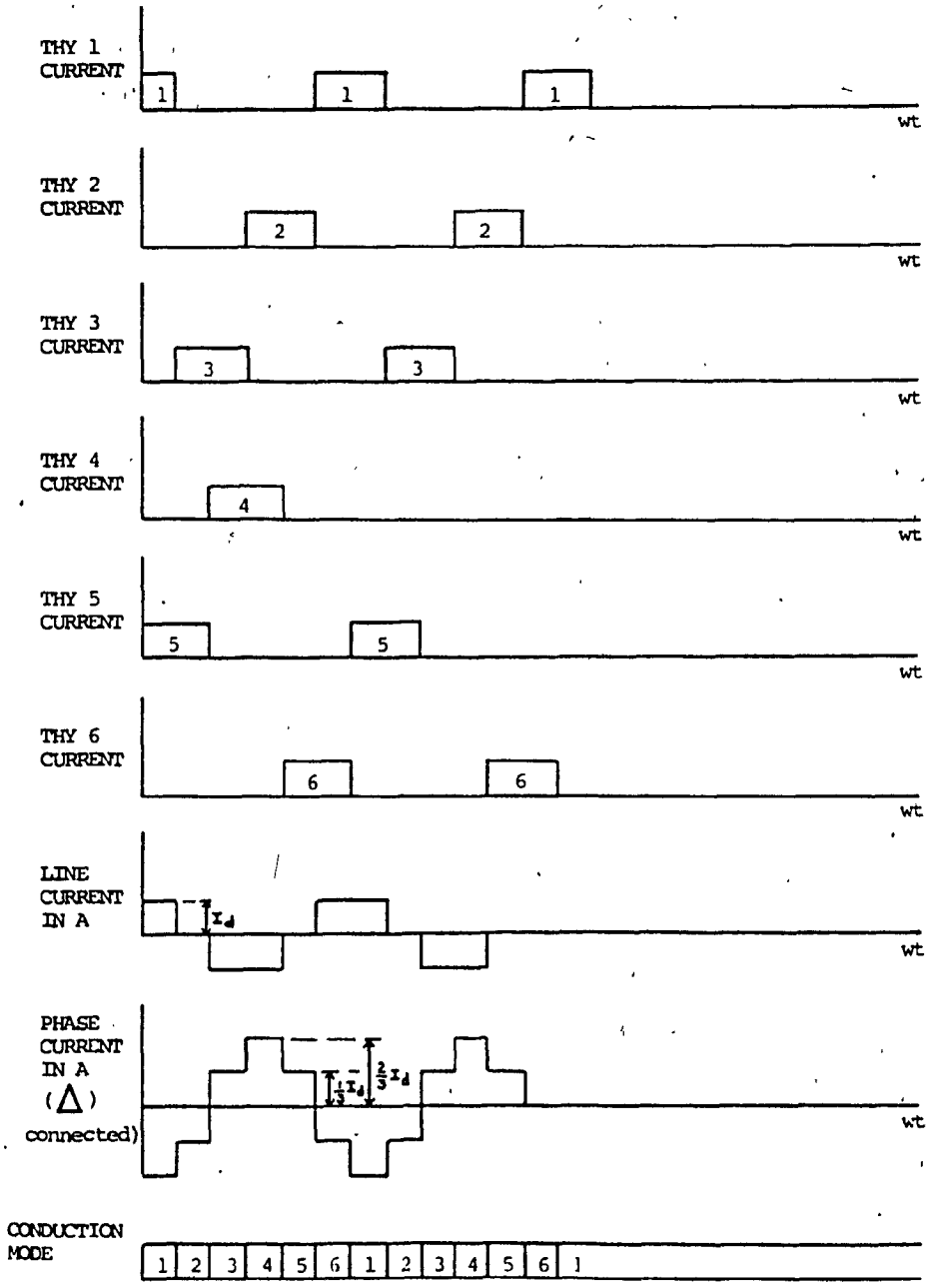

FIG. 2.16 THYRISTOR AND PHASE CURRENT IN CURRENT SOURCE INVERTER.

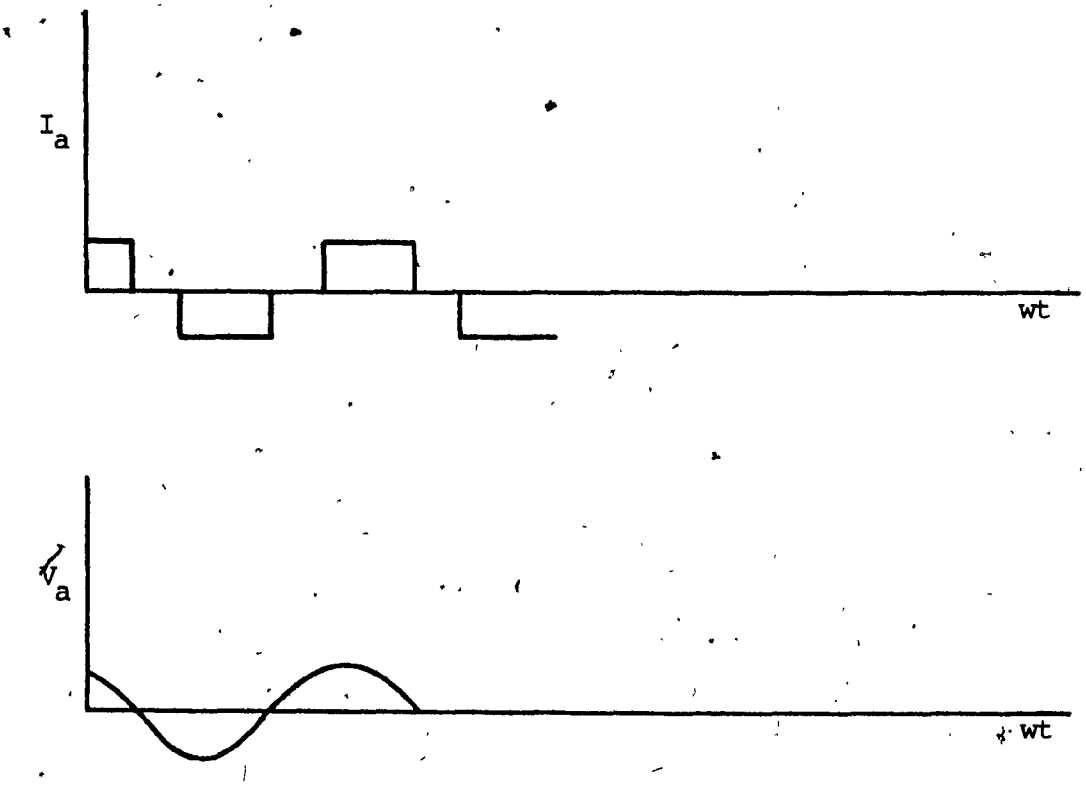

FIG. 2.17 PHASE V_a CORRESPONDING TO I_a.

MATHEMATICAL EXPRESSION

The corresponding Fourier series expressions for the phase current waveforms are given by:

$$I_a = I_{m1}\left[\sin w_1 t + \frac{1}{5}\sin 5\, w_1 t - \frac{1}{7}\sin 7\, w_1 t + \ldots\right] \quad \ldots 2.10$$

$$I_b = I_{m1}\left[\sin (w_1 t - \frac{2}{3}\pi) + \frac{1}{5}\sin (5\, w_1 t - \frac{2}{3}\pi) - \frac{1}{7}\sin (7 w_1 t - \frac{2}{3}\pi) + \ldots\right] \quad \ldots 2.11$$

$$I_c = I_{m1}\left[\sin (w_1 t - \frac{4}{3}\pi) + \frac{1}{5}\sin (5\, w_1 t - \frac{4}{3}\pi) - \frac{1}{7}\sin (7 w_1 t - \frac{4}{3}\pi) + \ldots\right] \quad \ldots 2.12$$

Corresponding voltage expressions are:

$$V_a = V_1 \sin (w_1 t - \theta_1) + V_5 \sin (5\, w_1 t - \theta_5) - V_7 \sin (7\, w_1 t - \theta_7) \quad \ldots 2.13$$

$$V_b = V_1 \sin (w_1 t - \frac{2}{3}\pi - \theta_1) + V_5 \sin (5\, w_1 t - \frac{2}{3}\pi - \theta_5) - V_7 \sin (7\, w_1 t - \frac{2}{3}\pi - \theta_7) \quad \ldots 2.14$$

$$V_c = V_1 \sin (w_1 t - \frac{4}{3}\pi - \theta_1) + V_5 \sin (5\, w_1 t - \frac{4}{3}\pi - \theta_5) - V_7 \sin (7\, w_1 t - \frac{4}{3}\pi - \theta_7) \quad \ldots 2.15$$

Where I_{m1} is:

$$I_{m1} = \frac{2}{\pi} I_d$$

2.4 Rectifier and inverter losses

While it is not the purpose of this thesis to investigate the rectifier and the inverter losses, it is useful to study them in order to have a better picture of the overall efficiency of the drive system. The classification of losses is the same for both rectifier and inverter. The only losses which are not common to them are commutation losses. The commutation losses due to the natural commutation of the thyristors in the bridge rectifier are absent. Classification of the losses is as follows:

1) Commutation losses (P_C)
2) Load losses (P_L)
3) Voltage losses (P_V)

2.4.1 Commutation Losses

Commutation losses consist of losses in the commutation thyristors, diodes, capacitors and inductors. Snubber circuit losses are also classified as commutation losses; however, they are treated separately. Due to the fact that their basic circuit configuration is the same, it is possible to obtain a general analysis.

Commutation Circuit Losses

Commutation is a process by which the current is diverted from one conducting path to another path making the first nonconducting. The commutation process depends on different types of circuit configuration. For this reason, it is difficult to find a general solution to calculate losses in commutation circuits. Therefore, a unique solution should be sought for

each commutation circuit. It is important to note that commutation circuit in inverters are a function of the power 3 . Commutation methods are divided into:

1) Natural commutation, also called load or line commutation.
2) Forced commutation.

Some of the most common forced commutation circuits are listed below:

1) Transformer commutated inverter.
2) Capacitor commutated inverter.
3) Transformer commutation with capacitor help.
4) MacMurray circuit, resonant commutation.
5) Mixed commutation inverter.

Andrew J. Humphrey[3] has classified the above into voltage or series commutation, and better path or parallel commutation.

Voltage or series commutation is a kind of commutation in which a voltage is connected in series with the load forcing the current into a more difficult path. Fig. 2.18, Fig. 2.20 and Fig. 2.22 are examples of voltage commutation. In Fig. 2.18 current is diverted directly from the load into the diode whereas in Fig. 2.20 the load current is first forced into a capacitor and then transferred into the diode. Figure 2.19 and Figure 2.21 are examples of better commutation. In Fig. 2.19, load current is trans-

ferred into a better path (auxiliary path) through the help of the charged capacitor.

Table 2.6 compares capacity and energy losses for Figures 2.18 through 2.22 in a three-phase bridge scheme.

CIRCUIT	CAPACITORS NUMBER	SIZE	VOLTAGE	VOLTS-FARADS	MINIMUM LOSS
Fig. 2.18	6	C	2E	12CE	$2CE^2$
Fig. 2.19	3	C	E	3CE	$0.5CE^2$
Fig. 2.20	6	C	1.5E	9CE } 15CE	$1.12CE^2$
	6	C	E	6CE }	
Fig. 2.21	3	C	E	3CE	$0.25CE^2$
Fig. 2.22	6	2C	E	12CE	CE^2

TABLE 2.6 CAPACITY AND ENERGY LOSS COMPARISON, THREE-PHASE BRIDGE.

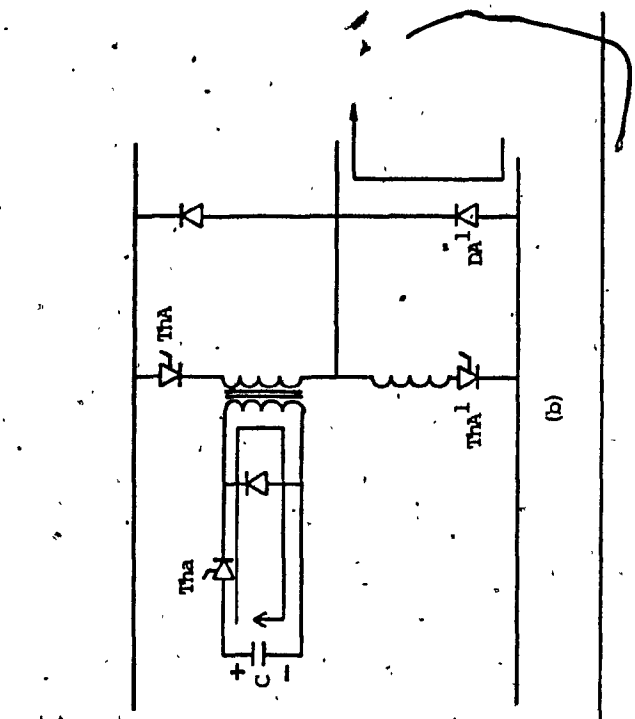

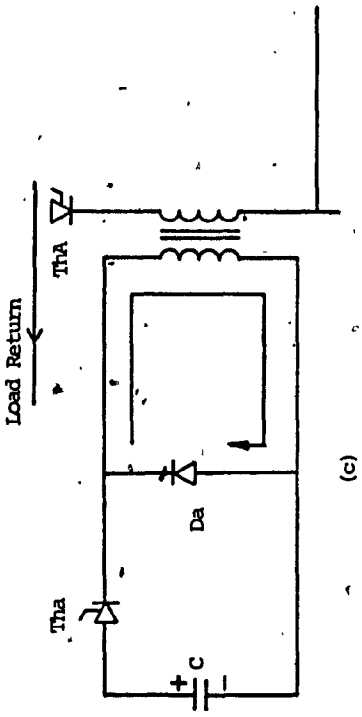

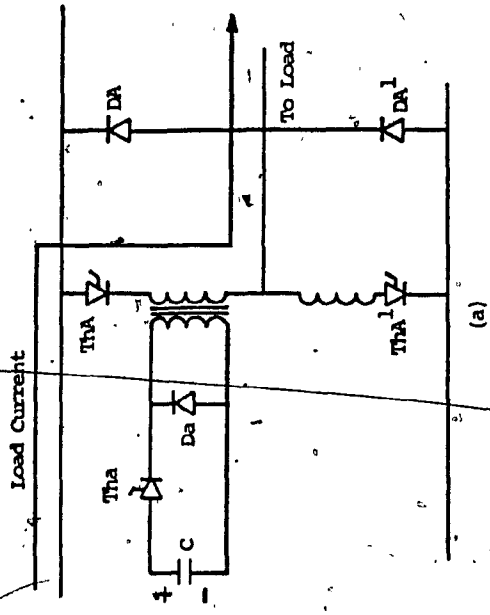

FIG. 2.18 TRANSFORMER COMMUTATED INVERTER.

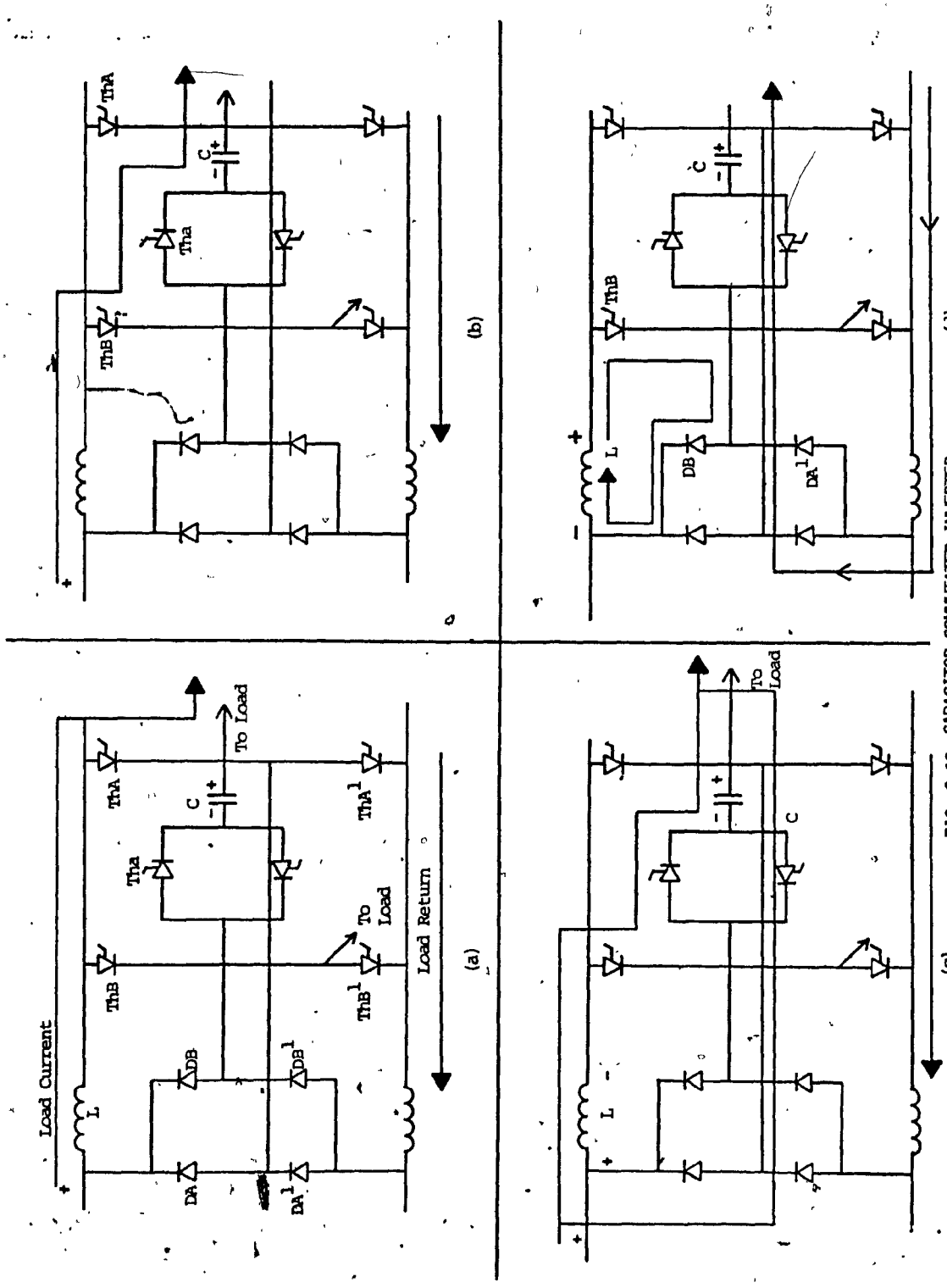

FIG. 2.19 CAPACITOR COMMUTATED INVERTER.

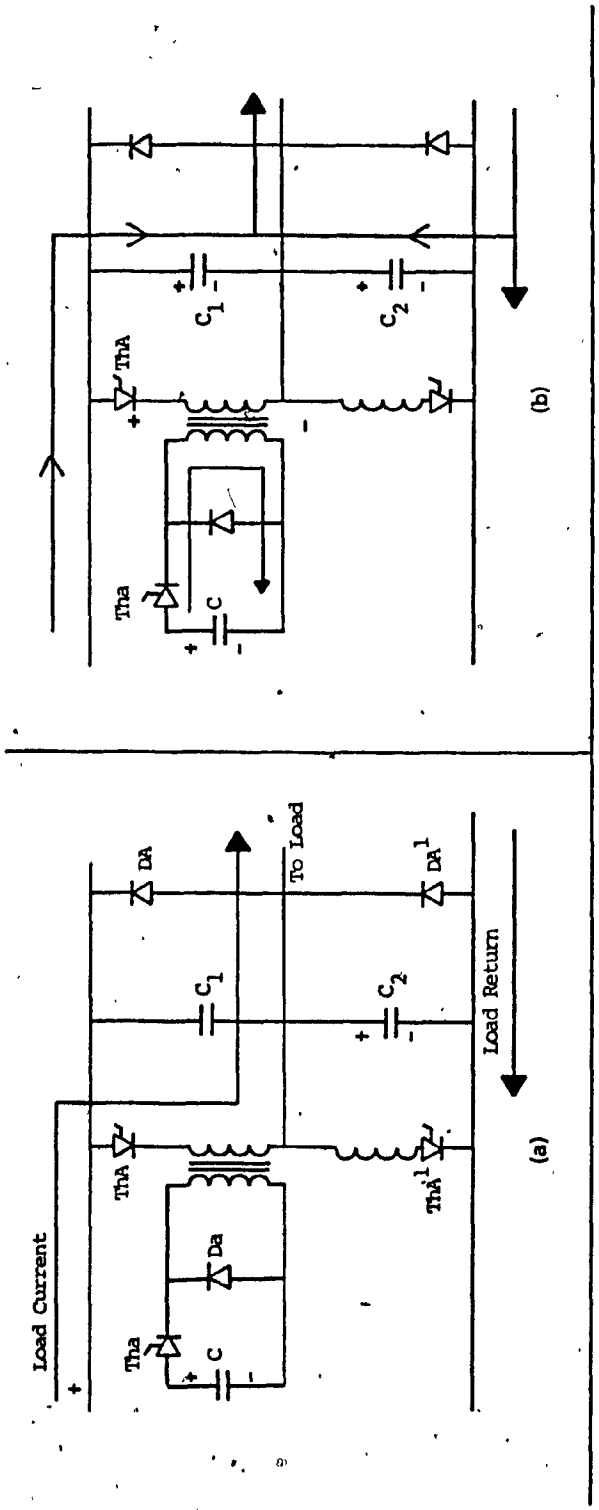

FIG. 2.20 TRANSFORMER COMMUTATION WITH CAPACITOR HELP.

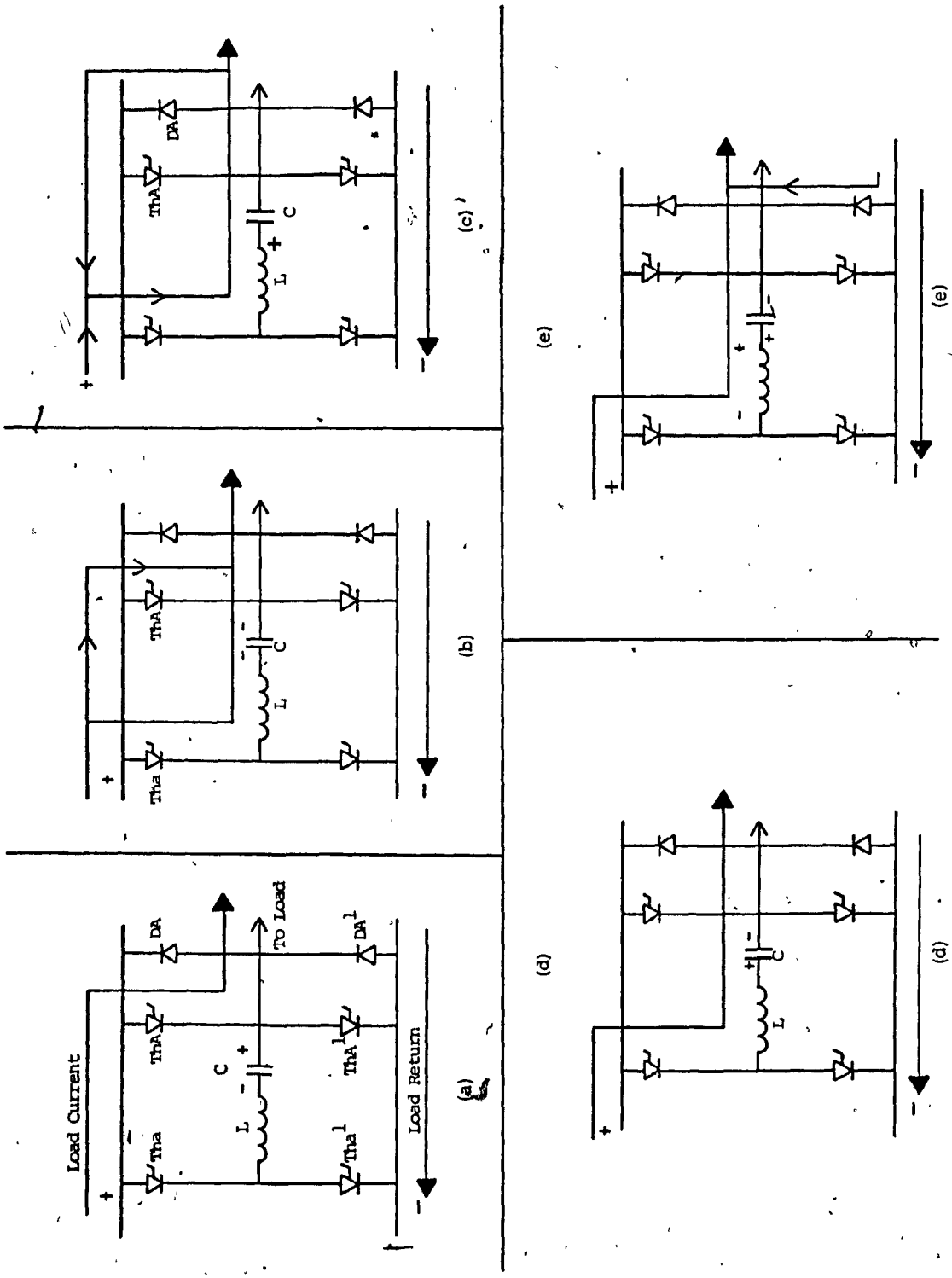

FIG. 2.21, MAC MURRAY CIRCUIT, RESONANT COMMUTATION.

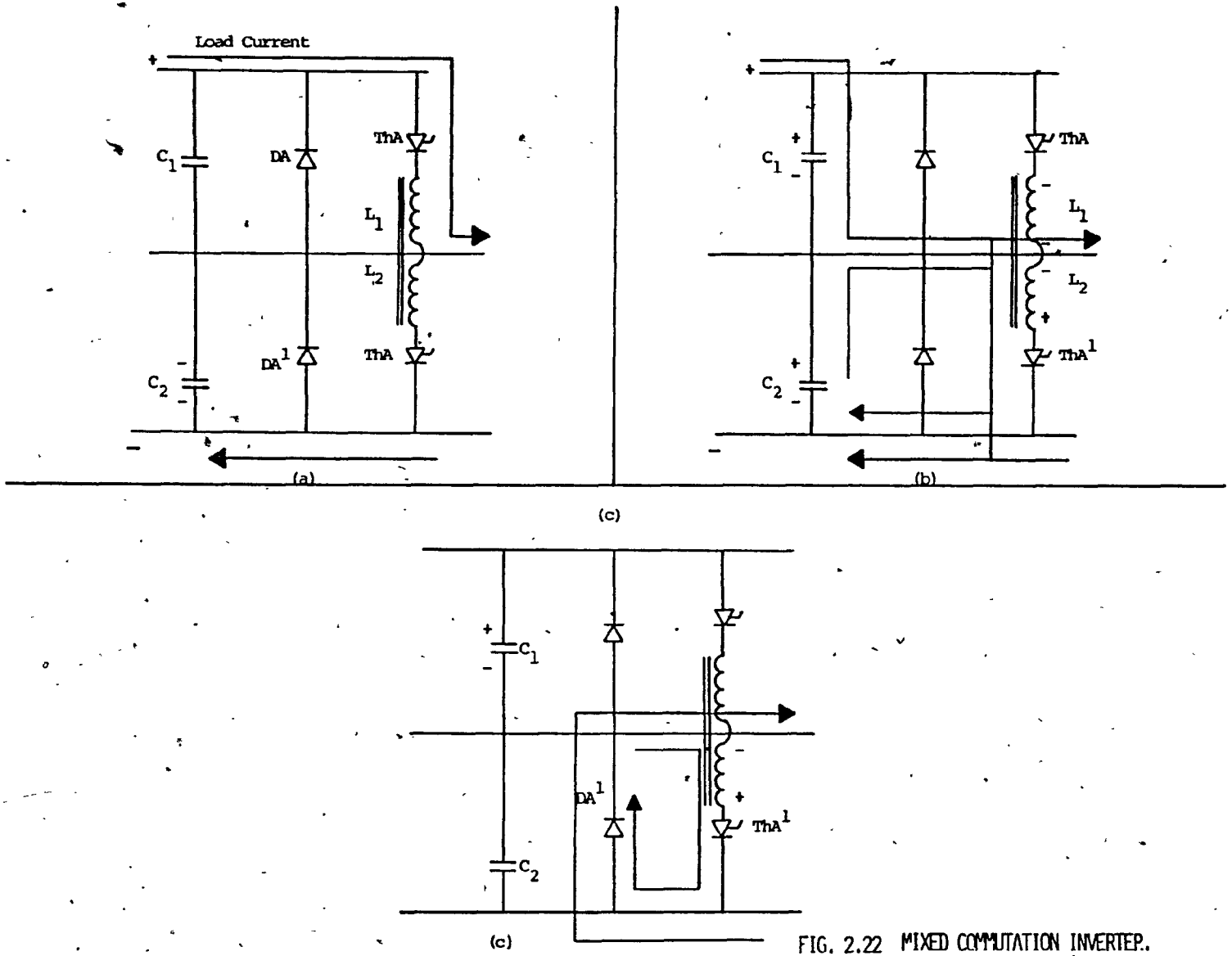

FIG. 2.22 MIXED COMMUTATION INVERTER.

2.4.2 Snubber Losses

Snubbers are protective RCL auxiliary circuits used as an aid to commutation. They may be connected across the transformer secondary and across the thyristors. Snubbers across the transformer are required if and only if there is not enough inductance between transformer and rectifier. The basic RLC circuit is shown in Fig. 2.23 . The objective of the inductor is to limit $\frac{di_{TH}}{dt}$ to an acceptable value. The objective of the capacitor is to limit $\frac{dv_{TH}}{dt}$ . . to an acceptable value. The resistor provides damping.

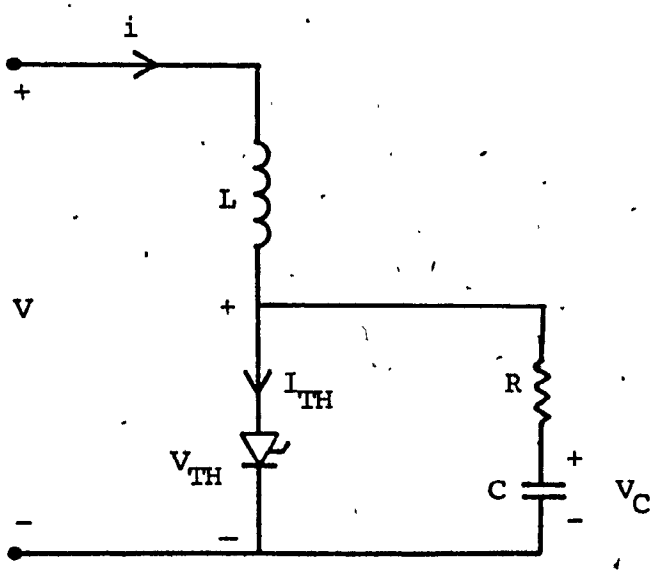

FIG. 2.23 BASIC SNUBBER CIRCUIT.

Before investigating snubber losses, it is necessary to analyse snubber operation modes. Total snubber losses are then the sum of all the losses occurring in each mode of operation. In order to analyse these modes of operation, certain assumptions have to be made. These assumptions have been summarized by T.H. Barton, [7]. Modes of operation in the snubber process are realized as follows:

1) Thyristor turn-on
2) Thyristor turn-off
3) Thyristor off and voltage discontinuities
4) Thyristor and sinusoidal excitation.

The analysis of the modes of operation is given in [7]. The associated losses are given in table 2.7.

MODES	LOSS EXPRESSION
1	negligible - zero
2+3	$V=\frac{1}{2}C(V_o-V_{co})^2+\frac{1}{2}LI_o^2$
4	$V=\int_{T_1}^{T_2} i^2 R_{dt}$

TABLE 2.7 SNUBBER LOSSES EXPRESSION.

Where:

V_o = line voltage = V_b-V_a

V_{co} = Initial Capacitor voltage

I_o = Reverse recovery current

i = Current passing through thyristor

CHAPTER 3

NON-SINUSOIDAL OPERATION OF 3-PHASE INDUCTION MOTORS

3.1 Introduction

The Interaction between a 3-phase induction motor and an inverter power supply results in additional losses, torque fluctuations, and possible instability, Fig. 3.1. Increased losses and torque fluctuation are the results of the inherent harmonic content in nonsinusoidal wave forms. Instability on the other hand, may be due to either inherent low frequency performance of the motor itself or the interaction between inverter and motor.

This chapter compares the performance of an induction motor when it is operated by a nonsinusoidal power supply to that of normal sine-wave supply. The comparison is carried out for a voltage source inverter; however, the same procedure is equally applicable to a current source inverter.

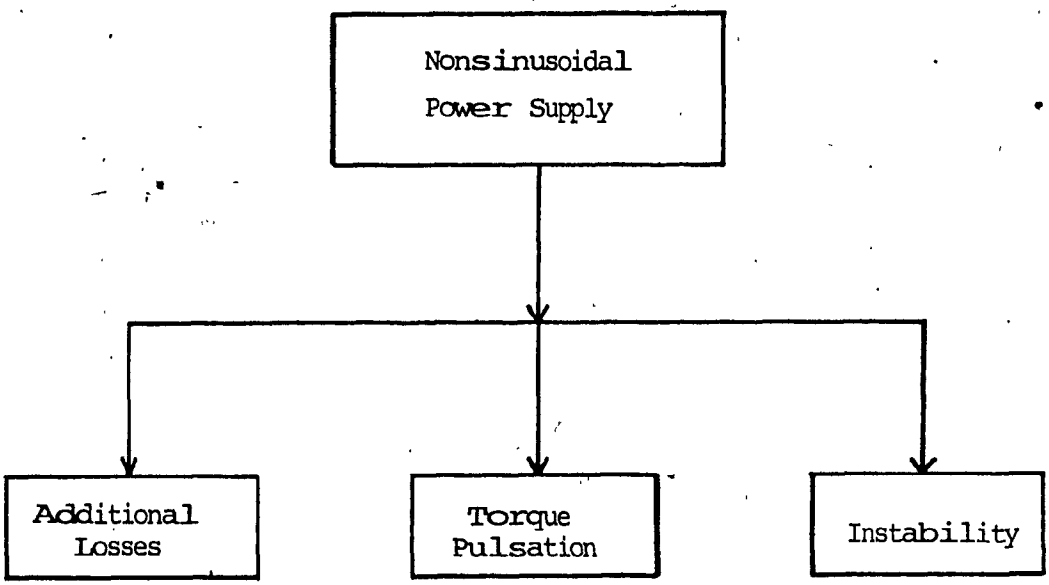

FIG. 3.1 DISADVANTAGES OF USING NONSINUSOIDAL POWER SUPPLIES.

3.2 Magnomative force

The m.m.f. harmonics produced in the air gap of the motor are divided into:

a) Space harmonic m.m.f waves.

b) Time harmonic m.m.f waves.

Both types are present simultaneously in the air gap.

3.2.1 Space harmonic m.m.f. waves

The stator winding is distributed in a series of slots built in the iron surface. For this reason, the spatial m.m.f. distribution is not sinusoidal. Therefore, a Fourier series analysis may be applied to express the spatial m.m.f. in terms of its fundamental and harmonic components. The fundamental components for a typical winding are given below, but these depend on the layout of the particular winding.

$$F_a = I_1 \cos\delta \sin \omega t \qquad \ldots\ldots 3.1$$

$$F_{b\phi} = I_1 \cos\left(\delta - \frac{2\pi}{3}\right) \sin\left(\omega t - \frac{2\pi}{3}\right) \qquad \ldots\ldots 3.2$$

$$F_c = I_1 \cos\left(\delta - \frac{4\pi}{3}\right) \sin\left(\omega t - \frac{4\pi}{3}\right) \qquad \ldots\ldots 3.3$$

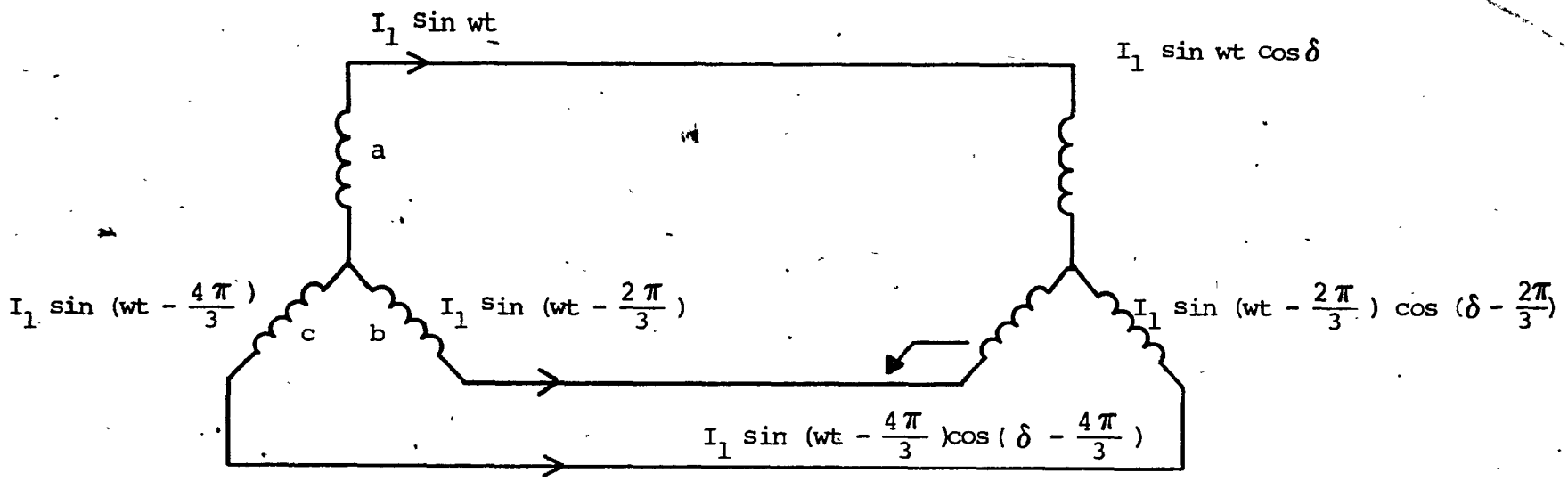

FIG. 3.2 3-PHASE INDUCTION MOTOR WITH SINUSOIDAL WINDING SUPPLIED FROM SINUSOIDAL SOURCE.

The three phase power supply currents are out of phase by 120° in time. Each phase current produces an m.m.f. The resulting m.m.f.s are out of phase by 120° in space, Fig. 3.2. Algebriaic combinations of the three fundamental m.m.f. waves yields:

$$f = \frac{3}{2} I_1 \sin (wt - \delta) \quad \ldots\ldots 3.4$$

Equation 3.4 states that the m.m.f. has a constant amplitude and travels with angular velocity of w in the increasing direction of δ.

This implies that sin (wt - δ) must be constant. In order for sin (wt - δ) to be constant, (wt - δ) must be constant. Differentiating (wt - δ) with respect to time yields:

$$\frac{d\delta}{dt} = w \quad \ldots\ldots 3.5$$

This angular velocity is the synchronous speed.

The fifth harmonic m.m.f. due to phase one is:

$$F_a = I_{5a} \cos 5\delta \sin wt \quad \ldots\ldots 3.6$$

When the corresponding expressions for f_2 and f_3 have been added to f_1, the result is as follows:

$$f = \frac{3}{2} I_{5a} \sin (wt + 5\delta) \quad \ldots\ldots 3.7$$

From equation 3.7, it can be seen that the fifth spatial m.m.f travels in the opposite direction of the fundamental spatial m.m.f. at a constant speed equal to $\frac{1}{5}$ of the synchronous speed.

A similar analysis shows that the seventh m.m.f. harmonic travels in the same direction as the fundamental at a constant speed equal to $\frac{1}{7}$ of the synchronous speed.

3.2.2 Time harmonic m.m.f.

Let us assume only the fundamental space m.m.f. is present in the air gap. Now consider an AC motor operated by a nonsinusoidal supply. As mentioned previously, the nonsinusoidal wave contains a significant number of harmonics. These harmonics, like the fundamental, set up an m.m.f. in the air gap. Consider, for example, the fifth harmonic phase current in coil one. It produces the following m.m.f:

$$f_1 = I_{1,5} \cos\delta \sin 5\,wt \qquad \ldots\ldots 3.8$$

The corresponding m.m.f. in the other two coils are the same apart from the fact that they are out of phase by 120° in space with respect to each other. The combination of the produced m.m.f's results

$$f = \frac{3}{2} I_{1,5} \sin (5\,wt + \delta) \qquad \ldots\ldots 3.9$$

Equation 3.9 shows that the fifth harmonic m.m.f. rotates in the opposite direction to the fundamental component with a constant speed equal to five times of the synchronous speed.

ORDER OF SPACE HARMONIC (h)	ORDER OF TIME HARMONIC (ν)						
	1	3	5	7*	9	11	13
1	+1	-	-5	+7	-	-11	+13
3	-	± 1	-	-	± 3	-	-
5	$-\frac{1}{5}$	-	+1	$-\frac{7}{5}$	-	$+\frac{11}{5}$	$-\frac{13}{5}$
7	$+\frac{1}{7}$	-	$-\frac{5}{7}$	+1	-	$-\frac{11}{7}$	$+\frac{13}{7}$
9	-	$\pm\frac{1}{3}$	-	-	± 1	-	-
11	$-\frac{1}{11}$	-	$+\frac{5}{11}$	$-\frac{7}{11}$	-	+1	$-\frac{13}{11}$
13	$+\frac{1}{13}$	-	$-\frac{5}{13}$	$+\frac{7}{13}$	-	$-\frac{11}{13}$	+1
15	-	$\pm\frac{1}{5}$	-	-	$\pm\frac{3}{5}$	-	-

TABLE 3.1 M.M.F. COMPONENTS OF A THREE PHASE ARMATURE WINDING.

Applying the calculations on the previous pages for the other higher harmonics results in the following conclusion. The m.m.f. wave of the order $k = 3n + 1$ where $n = 0,1,2, \ldots$ travel in the same direction as the fundamental component, whereas m.m.f. waves of the order $k = 3n + 2$ travel in the opposite direction of the fundamental component.

3.2.3 Combined space and time harmonics

Both space and time harmonics may be present simultaneously in the air gap. The presence of time harmonics of m.m.f. also results in some other space harmonics. This is summarized in table 3.1, where positive signs refer to those m.m.f. waves which travel in the same direction as the fundamental component (positive sequence). Negative signs refer to those m.m.f. waves which travel in the opposite direction of the fundamental component (negative sequence). Zeros refer to the third and multiples of the third harmonic (zero sequence).

3.3 Nonsinusoidal Behaviour of Induction Motors

If magnetic saturation is assumed to be negligible in an induction motor, then the induction motor could be considered as a linear device. In such a case, the superposition principal may be applied to calculate the total response of the motor. This response is the sum of the fundamental and the harmonic excitations.

An equivalent circuit of the induction motor must be derived as the basis for the calculation of quantities such as losses, steady state torque. The conventional fundamental equivalent circuit of an induction motor is shown in Fig. 3.3.

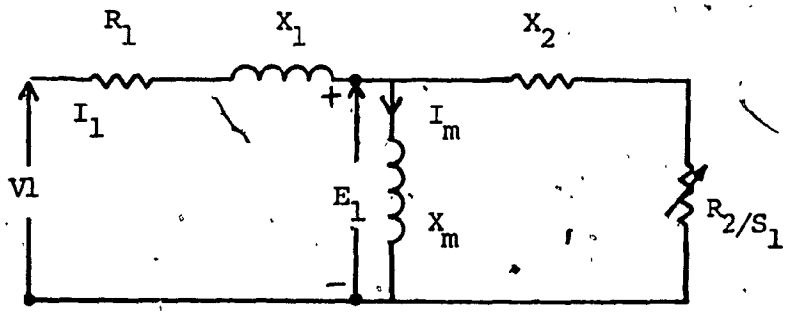

Fig. 3.3: The fundamental equivalent circuit of an induction motor.

Where:

R1 and R2 are stator and rotor resistances respectively.

X_1 and X_2 are stator and rotor leakage reactances.

X_m is the magnetization reactance.

s_1 is the fundamental slip of rotor with respect to stator.

$$s_1 = \frac{n - n1}{n} \qquad \ldots\ldots 3.10$$

where:

n is the synchronous speed

n_1 is the rotor speed

The equivalent circuit in Fig. 3.3 must be modified as shown in Fig. 3.4 in order to account for the harmonic contributions. The harmonic slip in Fig.3.4 is equal to:

$$S_\nu = \frac{\nu \pm (1-S1)}{\nu} \qquad \ldots\ldots 3.11$$

where ν is the order of harmonic [10]. The positive sign indicates the rotor is moving in the opposite direction of synchronous speed, and the negative sign indicates the rotor is travelling in the same direction as the synchronous speed.

Where:

$R_{l1\nu}$ is harmonic leakage stator resistor.

$R_{m1\nu}$ is harmonic magnetic stator resistor.

$R_{l2\nu}$ is harmonic leakage rotor resistor.

$R_{m2\nu}$ is harmonic magnetic rotor resistor.

$R_{2\nu}$ is harmonic rotor resistor.

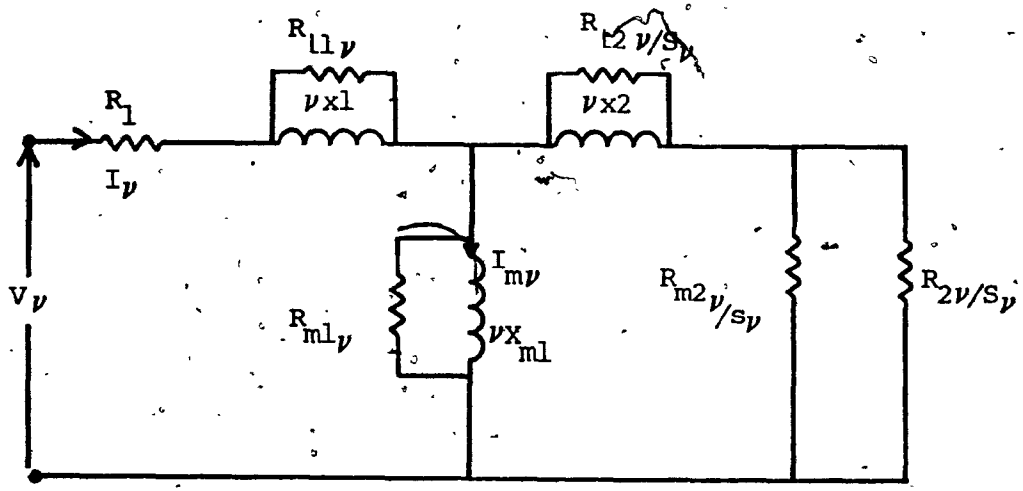

FIG. 3.4 EQUIVALENT HARMONIC CIRCUIT OF AN INDUCTION MOTOR.

The equivalent circuit of 3.4 emphasizes the fact that

1) The rotor, and stator resistances become larger at higher frequencies due to the skin effect.

2) The speed variation does not affect the harmonic slip very much. Consider, for example, S_1 varies from 0 to 1. Corresponding variation in S_5 and S_7 are 1.2 to 1 and .857 to 1 respectively. At higher frequencies, S_ν is even closer to unity. As a result, the equivalent of Fig. 3.4 could be simplified further to that of Fig. 3.5.

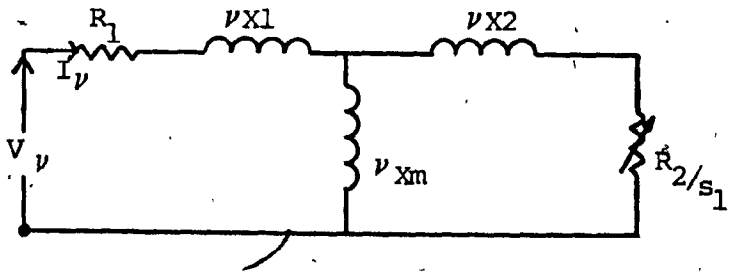

Fig. 3.5: Illustrates the small effect of speed variation.

The inductive reactances increase directly with the frequency. The rotor resistance increases with frequency but the increase is much less than that of the reactances and as a result, it may be neglected in comparison with the value of reactance at harmonic frequencies. This simplifies the Fig. 3.5 to Fig. 3.6.

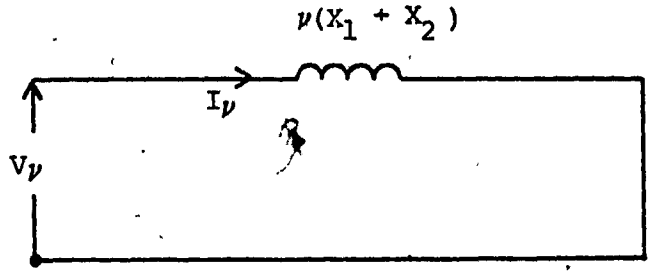

Fig. 3.6 Shows the effect of frequency.

Magnetization reactance has also been neglected in Fig. 3.6. Since it is much higher than the leakage reactances. Note that the equivalent circuit in Fig.3.6 is not valid for supply frequencies of less than 10 Hz. This reduced circuit is valuable when an approximate value of current is required because of its simplicity.

Harmonic Currents

A nonsinusoidal voltage power supply produces higher harmonic currents in the stator of the induction motor. In order to calculate harmonic currents, one must first calculate the harmonic impedances of the induction motor. Let V_ν denote the νth harmonic voltage and Z_ν the νth harmonic impedance. The νth harmonic current is therefore:

$$I_\nu = \frac{V_\nu}{Z_\nu}, \quad I_{rms} = \sqrt{I_1^2 + I_{har}^2} \qquad \ldots\ldots 3.12$$

Where: I_{har} is the rms value of the total harmonic content.

As mentioned earlier, S_ν is close to unity and the equivalent circuit of Fig. 3.5 is independent of speed. This indicates that the harmonic currents remain virtually unchanged under the whole speed range.

From equation 3.12, it is evident that if the leakage reactance of the motor is low, care must be taken when it is operated on a nonsinusoidal supply. Harmonic currents may cause excessive losses leading to an unacceptable temperature rise.

Experience has shown that current harmonics are inversely proportional to per unit reactance X_{pu} [12].

$$I_\nu = \frac{1}{\nu^2 X_{pu}} \qquad \ldots\ldots 3.13$$

where:

X_{PU} is per unit reactance at fundamental frequency and is given by

$$X_{PU} = \frac{I_{FL}}{I_s} \sin \theta_s \qquad \ldots\ldots 3.14$$

where:

I_s is the standstill stator current.

θ_s is the standstill displacement angle.

I_{FL} is full load current.

Fig. 3.7 illustrates the harmonic currents versus per unit reactance of a typical motor when fed by a six and a twelve-step voltage waveforms.

It is clear that the twelve-step r.m.s. current is negligible whereas the Six-step r.m.s. current is quite significant. For an induction motor with X_{pu} ranging from 0.1 to 0.2, the total r.m.s. current varies from 2 to 10 percent more than the fundamental one at full load. [12].

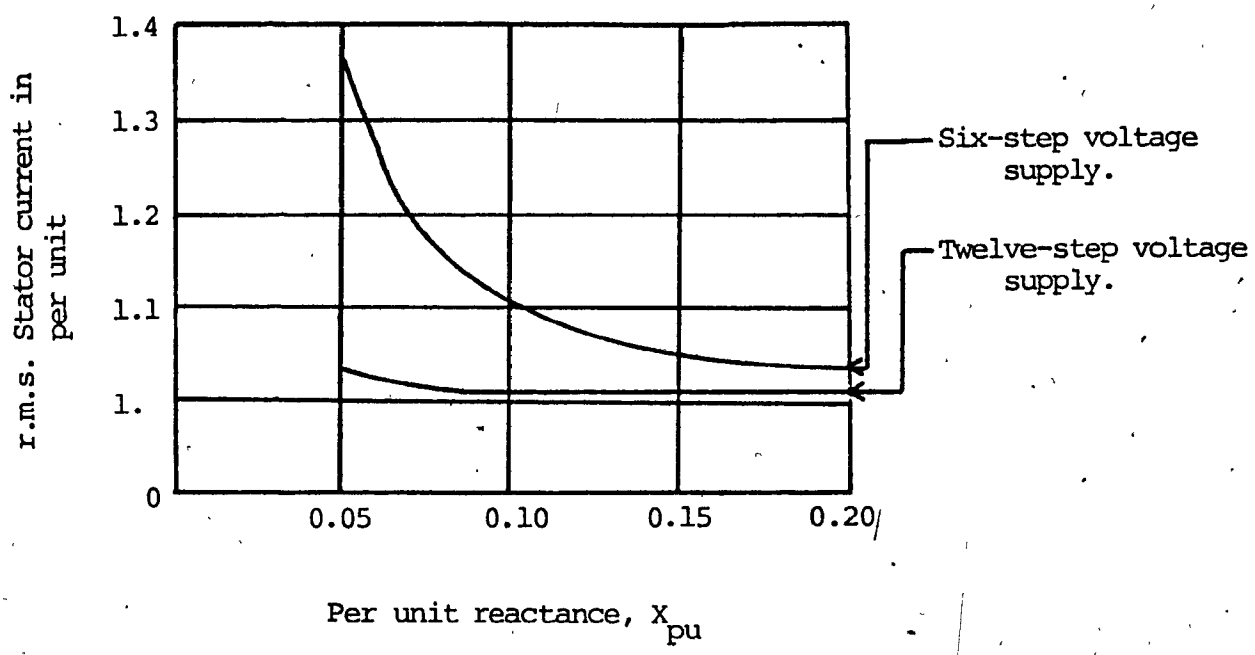

FIG. 3.7 STATOR CURRENT AS A FUNCTION OF PER UNIT LEAKAGE REACTANCE OF THE MOTOR.

To illustrate the difference in harmonic content between a Six-step voltage supply and a twelve-step voltage supply consider Fig.3.8, and Fig.3.9. It must be noted that these graphs were calculated for an AC motor with per-unit reactance of 0.1 and assuming the fundamental voltage leads fundamental current by 60°. [12]

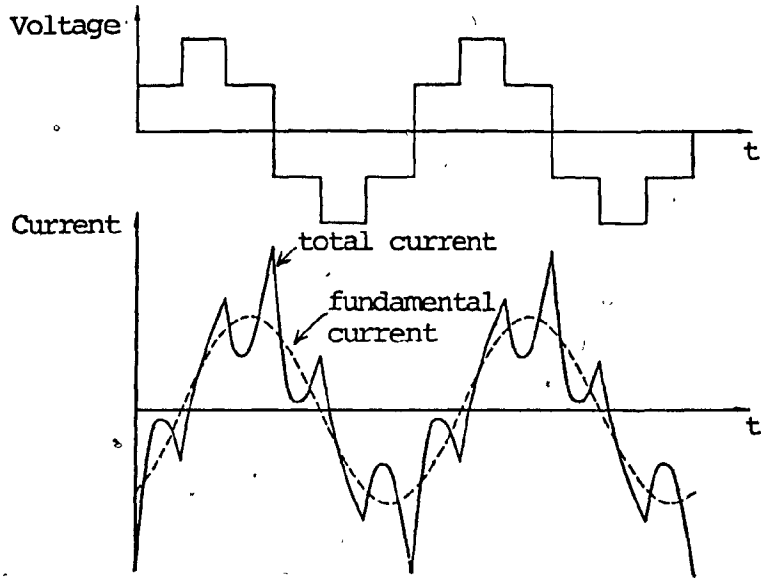

FIG. 3.8 STATOR VOLTAGE AND CURRENT WAVEFORMS FOR AN A.C. MOTOR WITH A SIX STEP VOLTAGE SUPPLY.

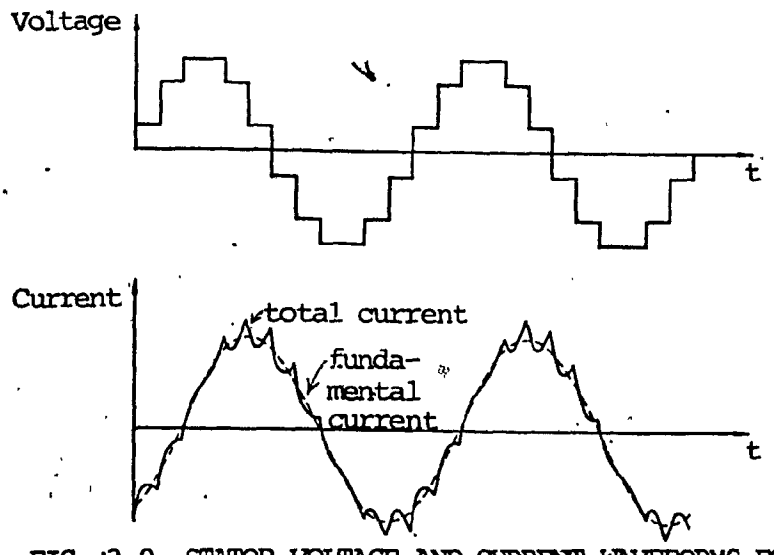

FIG. 3.9 STATOR VOLTAGE AND CURRENT WAVEFORMS FOR AN A.C. MOTOR WITH A TWELVE STEP VOLTAGE SUPPLY.

The harmonic distortion leads to two disadvantages. The first is an increase in the r.m.s. value of the stator current and the second is an increase in the current peaks which makes commutation more difficult. To show the second disadvantage, consider Fig.10. It shows how the improvement is accomplished by using a twelve-step voltage inverter. [12]

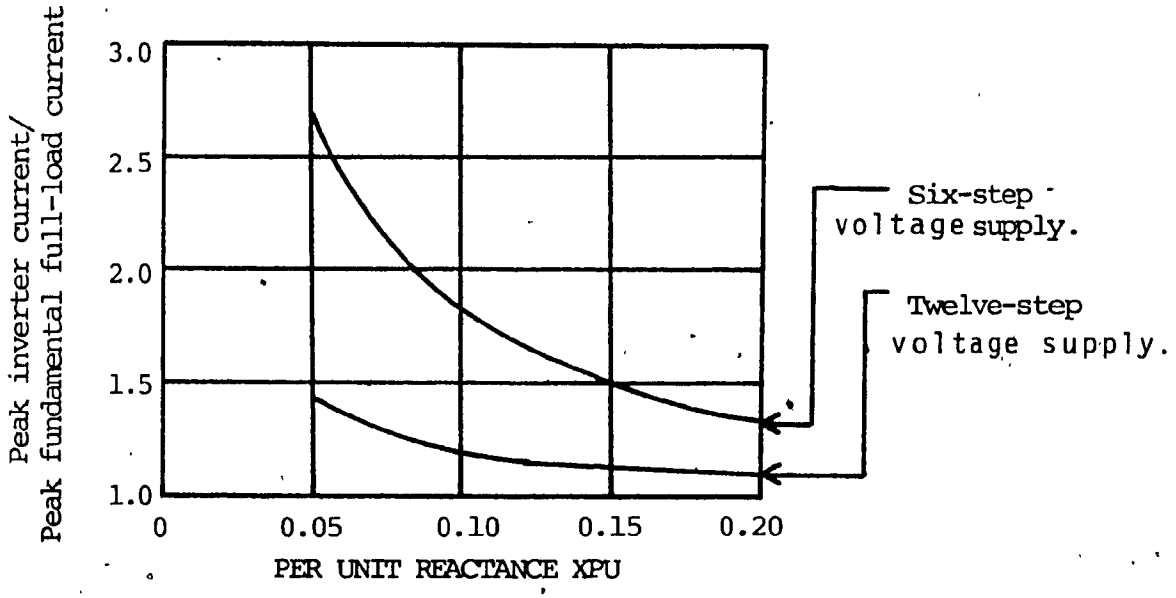

FIG. 3.10 PEAK INVERTER CURRENT AS A FUNCTION OF THE PER UNIT LEAKAGE REACTANCE OF THE MOTOR.

3.4 Harmonic Losses in the Squirrel-Cage Induction Motors

Nonsinusoidal waveforms produce additional losses in the Squirrel-Cage Induction Motor. They are classified as follows:

Copper Losses

1) The stator copper loss ($P_{cs\nu}$).
2) Rotor copper loss due to fundamental space field ($P_{cr\nu}$).
3) Rotor copper loss due to space harmonic fields. ($P_{cmn\nu}$).

Iron Losses

4) Iron loss in stator and rotor teeth due to space harmonic fluxes.
5) Iron loss due to end leakage flux.
6) Iron loss in stator and rotor teeth due to skew leakage flux (for motor with skewed construction).
7) Iron loss in stator and rotor due to space fundamental flux and referred to as core loss.

Numbers 3-6 constitute stray losses. [10]

The expressions for the losses may be found in [8-10] as follows:

1) $$P_{cs\nu} = 3\, I_{1\nu}^2\, R_1 \qquad 3.15$$

2) $$P_{cr\nu} = 3\, I_{21\nu}^2\, R_{21\nu} \qquad 3.16$$

3) $$\begin{cases} P_{cmn\nu} = 3\left[\left|I_{2pm\nu} + I_{2m\nu}\right|^2 R_{2m\nu} + \left|I_{2pn\nu} + I_{2n\nu}\right|^2 R_{2n\nu}\right] \\ P_{c57\nu} = 3\left[I_{25\nu}^2\, R_{25\nu} + I_{27\nu}^2\, R_{27\nu}\right] \end{cases} \qquad 3.17$$

4) $$B_{sm\nu} = \frac{1.57\nu\left[\left|I_{mpm\nu}\,(jX_{pm\nu}) + I_{mm\nu}\,(jX_{mm\nu})\right|\right]}{4.44K_{wm}\,T_{ph}\,f_1\,A_{st}} \qquad 3.18$$

$$B_{rm\nu} = B_{sm\nu}\frac{A'_{rt}}{A_{st}} \qquad 3.19$$

5) $$W_e = 0.3m\,(I^2)\,x\left[\frac{1.6\,fmN^2D_1}{P^2\,10^7}\log\left(1 + \frac{A^2}{4Y_1Y_2}\right)\right] \qquad 3.20$$

6) The true loss in stator and rotor teeth due to skin leakage flux circulation is given in [8].

7) Iron loss in stator and rotor due to spare fundamental flux methods of calculation is given in [10].

where

I = rms current per phase

f = line frequency

m = number of phases

N = effective winding turns in sine per phase

D1 = air gap diameter

P = number of poles

A = slant distance in inches between the assumed center of the stator and rator peripheral currents.

Y_1 Y_2 = Axial distance between the stator and rotor end-current centers to the end of the laminated core.

When calculating the stator copper loss of a large motor, the skin effect in the conductors must be considered. This is due to the fact that the stator conductors in large motors have an appreciable depth. Experiments have also shown that in the presence of harmonics, the fundamental term increases slightly due to increased magnetization current.

From equation (3.16), it is evident that skin effect has to be considered, because it increases with frequency. $R_{21\nu}$ increases as a consequence of increased skin effect. To illustrate the above, consider the fifth and the seventh m.m.f. harmonics which induce the sixth harmonic rotor current. If the supply frequency is 60Hz, then the frequency of the sixth harmonic rotor current becomes 360Hz. The rotor resistance at this frequency increases due to the skin effect. Therefore, it can be concluded that losses due to the rotor are the most severe ones. However, by using conductors having low skin effect, and by controlling the saturation of magnetic paths, the rotor losses can be reduced.

The stray losses due to space harmonic fluxes are negligible. The main parts of the stray losses are due to the end and skew leakage fluxes. They are appreciably large at high frequencies. The end leakage occurs as the result of eddy-current loss in the end lamination. The end leakage loss occurs both in rotor and stator. Skewed leakage loss occurs only in Squirrel-Cage induction motors in which the rotor slots are skewed with respect to stator slots. Skewed flux losses can be reduced to zero by using zero skew.

The efficiency of the induction motor decreases as a result of increased losses. The reduction of efficiency has been explained graphically in (10). The efficiency can be improved by using a 12-step waveform inverter on an efficient induction motor. The efficiency of both induction motors and inverters varies from manufacture to manufacture. The efficiency variation also depends on the type of construction as well as the magnetic material which is used.

3.5 Harmonic Torques

Resultant additional torques due to inverter harmonics in an induction motor are of two types.

1) Steady Harmonic Torques
2) Pulsating Harmonic Torques.

The steady torques are the result of interaction between time harmonic currents and air gap fluxes of the same order, whereas the pulsating torques are the result of interaction between time harmonic currents and air gap fluxes of different order.

3.5.1 Steady Harmonic Torques

The steady torques derivation follows the same procedure as the fundamental one.

$$T_\nu = \frac{Pm}{2\pi f_1 \nu} (I_{2\nu})^2 \left(\frac{R_{2\nu}}{S_\nu}\right) \quad \ldots\ldots 3.21$$

where:

T_ν is the νth harmonic steady torque.

p is number of poles.

m is number of phases.

If the induction motor is operating near the synchronous speed at the full load, then the equation (3.21) would be simplified to:

$$T_\nu = \frac{\pm Pm}{2\pi f_1} (I_{2\nu})^2 \frac{R_{2\nu}}{(\nu \pm 1)} \quad \cdots\cdots 3.22$$

This is due to the small fundamental slip

$$S_\nu = \frac{\nu \mp 1}{\nu} \quad \cdots\cdots 3.23$$

The positive sign in equation 3.22 refers to the steady torques from field components travelling in the same direction as the fundamental whereas the negative sign refers to steady torques from components travelling in the opposite direction of the fundamental. Skin effect must be considered to calculate $R_{2\nu}$. The effect of steady torques over the fundamental are very small and they could be ignored.

3.5.2 Pulsating harmonic torques

Harmonic torque pulsations in the induction motor has a mean value of zero. However, their presence affects the speed of the motor at very low speed. The magnitudes of torque pulsations are normally very small. However, in some types of inverters, such as pulse width modulation which produce high harmonic content at certain frequencies, pulsating torques may be relatively large. The torque pulsations occur as the result of

interaction between harmonic rotating mutual fluxes with harmonic m.m.f.'s of different order. The chief pulsating torques are those due to interaction between fundamental flux with harmonic m.m.f.'s.

In order to investigate the torque pulsations in an induction motor fed by a six-step voltage waveform, consider the six-step voltage wave form of Fig.3.11.

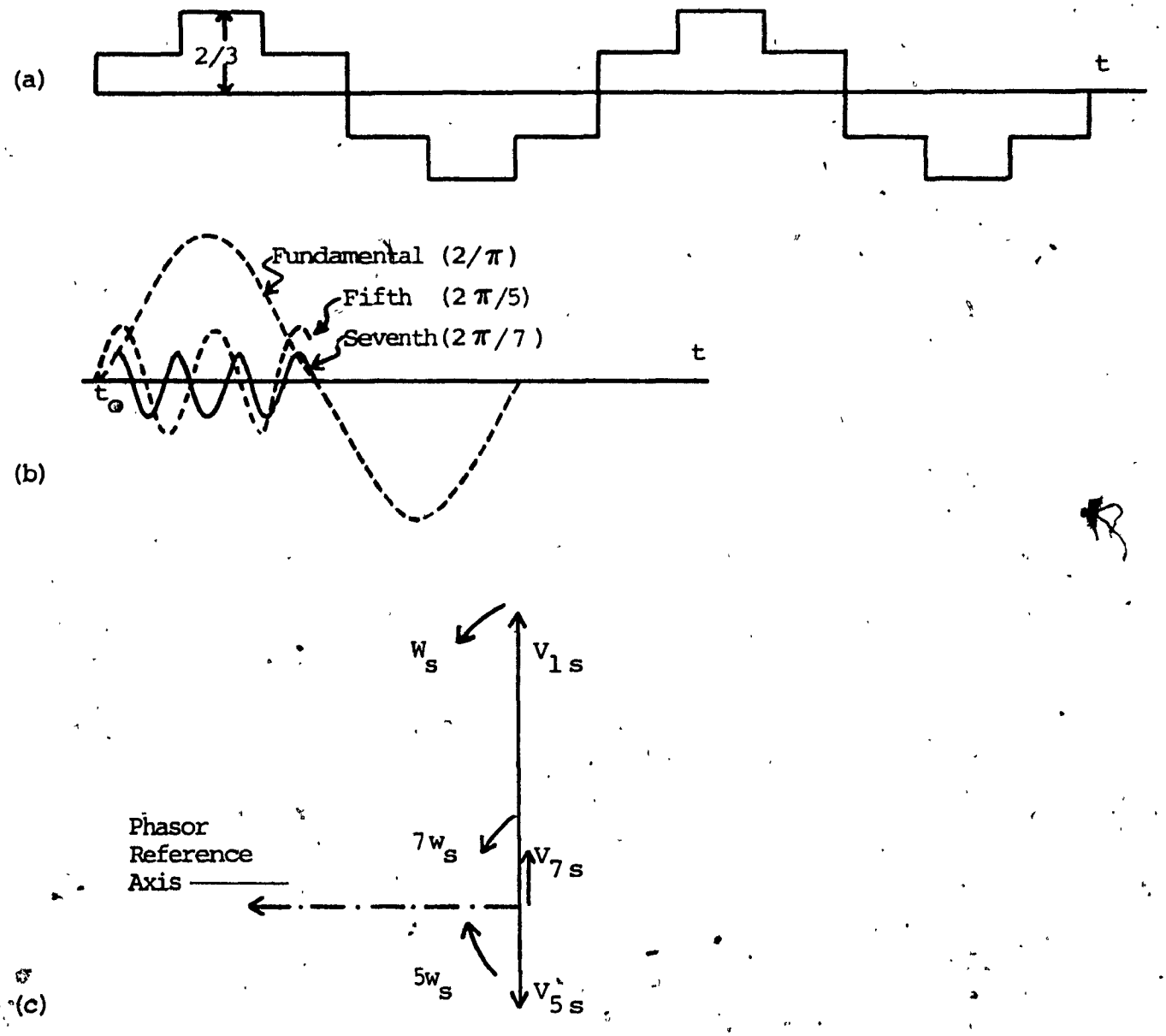

FIG.3.11 SIX-STEPPED WAVEFORM AND ITS FOURIER COMPONENTS (A) SIX-STEPPED VOLTAGE WAVEFORM. (B) FUNDAMENTAL, FIFTH, AND SEVENTH HARMONIC. (C) FUNDAMENTAL, FIFTH, AND SEVENTH HARMONIC PHASE VOLTAGE.

The phasors representing the m.m.f. ($I_{\nu r}$) and mutual flux quantities ($\phi_{\nu m}$), are illustrated in Fig.3.12. The sixth harmonic torque T_6 is the sum of the following two terms:

1) Interaction between ϕ_{1m} and the harmonic currents I_{5r} and I_{7r}.

2) Interaction between I_{1r} plus ϕ_{7m} and ϕ_{5m}.

The following formulates the above:

$$T_6 = -\phi_{1m}(I_{5r} - I_{7r}) \sin 6w_s t + I_{1r}(\phi_{5m} - \phi_{7m}) \cos 6w_s t. \quad \ldots\ldots 3.24$$

The calculation has shown that the amplitude of the second term is less than one fifth that of the first term. Hence equation 3.24 can be simplified to:

$$T_6 \simeq \phi_{1m}(-I_{5r} + I_{7r}) \quad \ldots\ldots 3.25$$

T_{12}, the twelfth harmonic torque, is obtained in the same manner as following:

$$T_{12} \simeq \phi_{1m}(-I_{11r} + I_{13r}) \quad \ldots\ldots 3.26$$

(a)

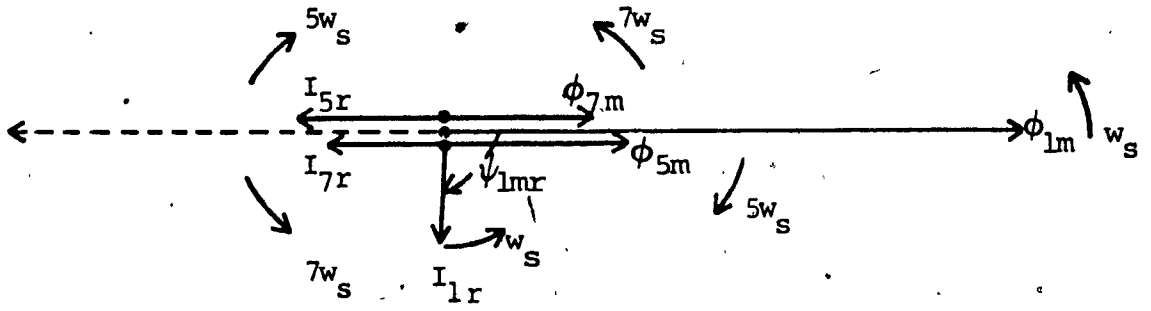

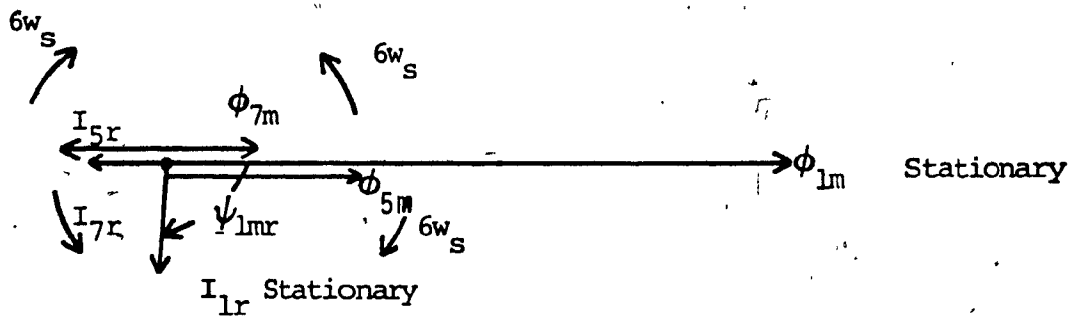

(b)

FIG. 3.12 (A) PHASOR DIAGRAM OF ϕ_{1m} AND I_{1r} AT SYNCHRONOUS SPEED w_s
(B) ϕ_{1m} AND I_{1r}, STATIONARY.

It is clear that T_{12} is much smaller than T_6. The torque fluctuations at higher frequencies are even much smaller. T_6 is the main torque pulsation which has to be considered.

Fig. 3.13 illustrates an Induction motor torque pulsation at no-load-rated torque and at twice-rated torque, fed from a six-step voltage supply. (11)

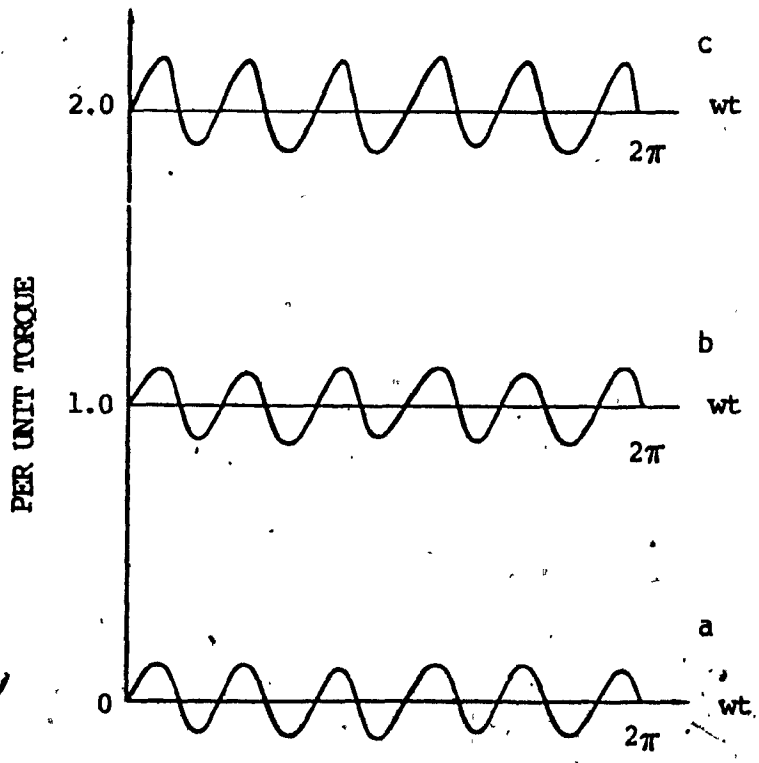

Fig. 3.13 Torque pulsation of an induction motor.

a) At no load

b) At rated torque

c) At twice-rated torque.

CHAPTER 4

COMPUTATIONAL RESULTS

This chapter contains the computational results obtained by four computer programs. These computer programs are as follows:

Voltage Source inverter wave (VSIW)

Current Source inverter wave (CSIW)

Voltage Source inverter fed induction motor (VSIFIM)

Current Source inverter fed induction motor (CSIFIM)

VSIW and CSIW are two programs written to plot the output voltage and current waveforms of VSI and CSI. They also compute the power factor as well as load losses.

The VSIW and CSIW are basically duals of each other. The VSIW demonstrates the output characteristics of a VSI power supply; whereas the CSIW demonstrates the output characteristics of a CSI. These are shown in Fig. 4.1 and Fig. 4.2.

The rectifier, inverter load losses, and power factor of VSI and CSI are given in Table 4.1.

VSIFIM and CSIFIM are two programs used to compute the various losses, efficiency, steady state torque, and torque pulsation of a typical

squirrel cage induction motor fed by VSI and CSI. In both programs the magnetization current is kept constant. This is to keep air gap flux constant for the sake of comparing the squirrel cage induction motor's performance fed from VSI and CSI. The equivalent circuit of (10) was used to demonstrate the effect of fundamental as well as higher harmonic components.

The computations were repeated for five different values of slip ranging from .01 to .06.

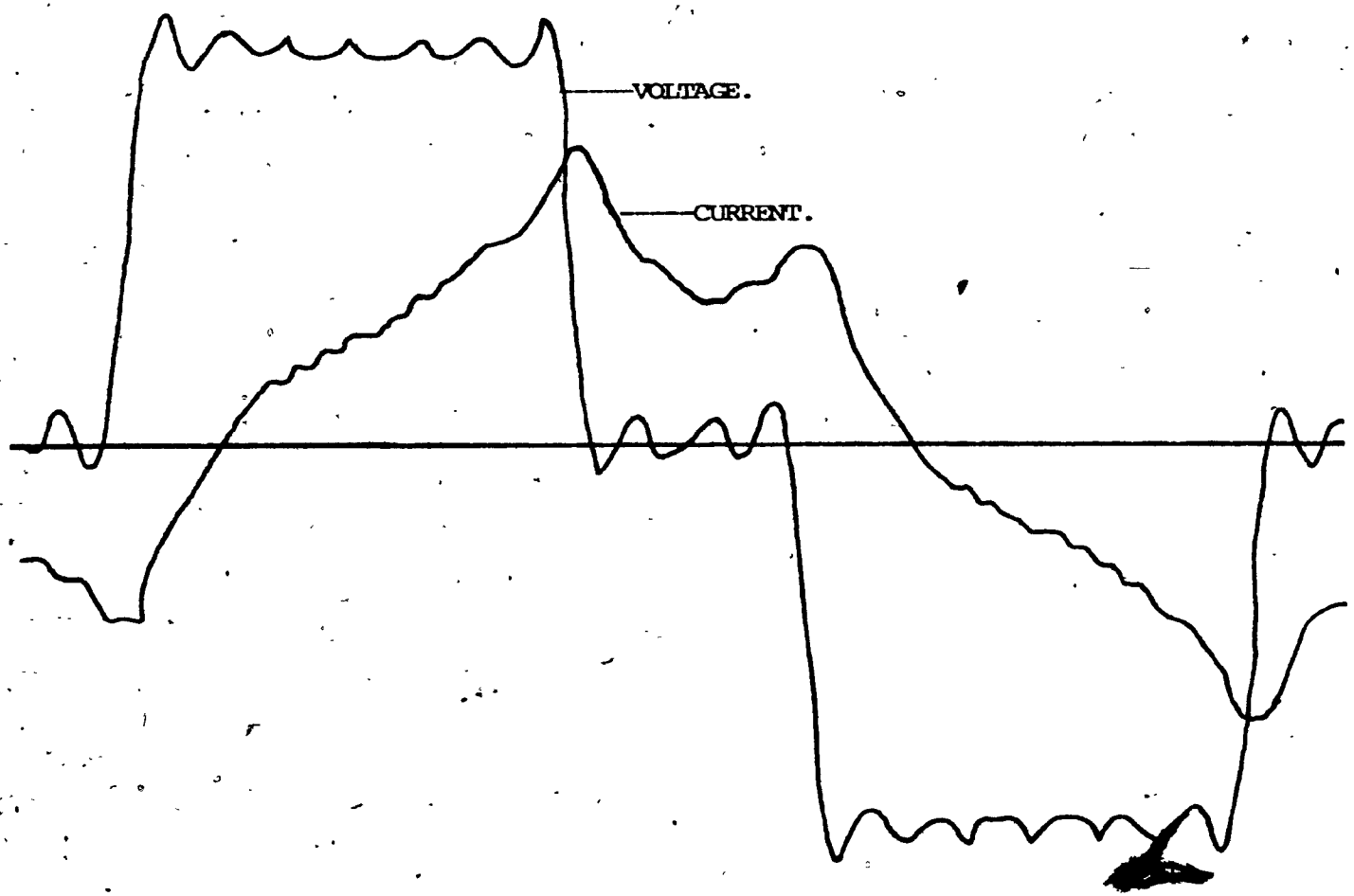

FIG. 4.1 THE OUTPUT LINE TO LINE VOLTAGE AND PHASE CURRENT OF A VSI.

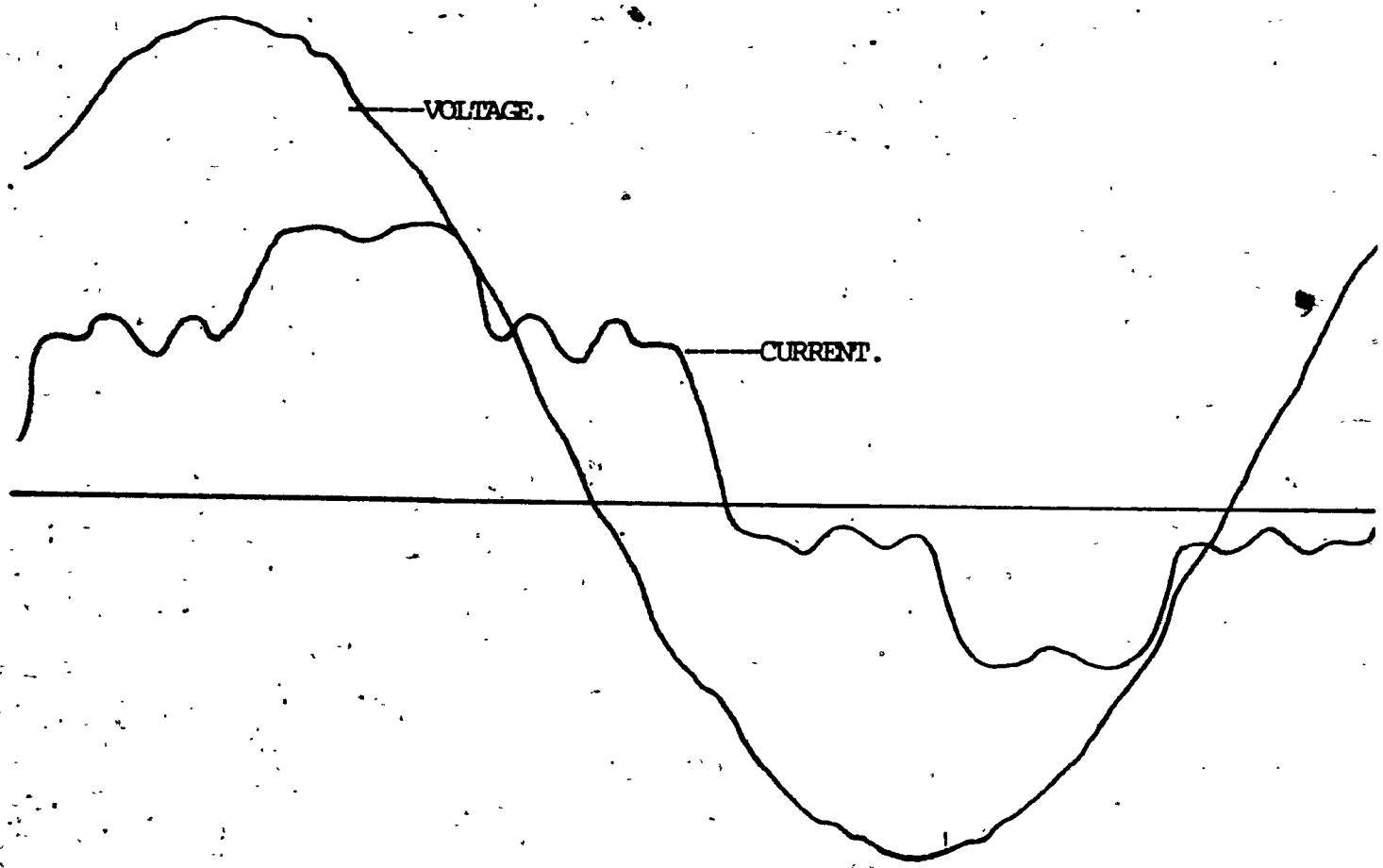

FIG. 4.2 THE OUTPUT LINE TO LINE VOLTAGE AND PHASE CURRENT OF A CSI.

POWER SUPPLY TYPE	RECTIFIER LOAD LOSSES	INVERTER LOAD LOSSES	DISTORTION POWER FACTOR
VSI	63.48W	41.2W	.99
CSI	78.33W	59.56W	.98

TABLE 4.1 Compares the load losses and input power factor of voltage and current source inverter.

WHERE:

The output line to line voltage for both VSI and CSI are equal to 200 volts. Forward voltage drop across each thyristors is .8 volts. Forward resistance of each thyristor is .7mΩ.

VARIABLE FREQUENCY POWER SUPPLY: CSI

HARM-ONIC ORDER	LOSS A	LOSS B	LOSS C	LOSS D	LOSS E	LOSS F	TOTAL LOSS HARMONIC
1	29.86254	3.53171	118.92476	.00174	.01189	2.24852	463.74344
5	1.19450	1.56436	.21820	.02300	1.00005	1.63829	13.91522
7	.60944	1.41490	.19873	.01645	.00003	.83491	9.22337
11	.24680	1.26265	.17971	.01808	.00001	.33835	6.13676
13	.17670	1.21328	.17490	.01530	.00001	.2405	5.46674
17	.10333	1.13435	.16852	.01661	.00000	.14150	4.69298
19	.08272	1.10004	.16634	.01487	.00000	.11319	4.43149
TOTAL LOSS	32.27603	11.22129	120.03116	.10605	1.01199	5.55526	507.609

EFFICIENCY: .49139

TABLE 4.2: The fundamental, harmonic losses and efficiency of the induction motor for slip = .01.

WHERE:
A is STATOR COPPER LOSS.
B is STATOR LEAKAGE FLUX LOSS.
C is STATOR MUTUAL FLUX LOSS.
D is ROTOR LEAKAGE FLUX LOSS.
E is ROTOR MUTUAL FLUX LOSS.
F is ROTOR COPPER LOSS.

VARIABLE FREQUENCY POWER SUPPLY: CSI

HARMONIC ORDER	HARMONIC STEADY TORQUE
1	5.36794
5	-.00653
7	.00332
11	-.00067
13	.00048
17	-.00019
19	.00015
TOTAL TORQUE	5.36450

TABLE 4.3: Steady Harmonic Torque.

Produced in the Induction Motor for SLIP= .01

VARIABLE FREQUENCY POWER SUPPLY: CSI

HARMONIC ORDER	LOSS A	LOSS B	LOSS C	LOSS D	LOSS E	LOSS F	TOTAL LOSS HARMONIC
1	35.08153	4.14893	114.85818	.01343	.04590	8.68028	488.4876
5	1.40326	1.83776	.25644	.05373	.00012	1.92436	16.42701
7	.71595	1.66218	.23353	.03852	.00006	.98070	10.89282
11	.28993	1.48332	.21114	.04224	.00002	.39738	7.27213
13	.20758	1.42532	.20549	.03581	.00002	.28428	6.47553
17	.12139	1.33260	.19796	.03882	.00001	.16616	5.57083
19	.09718	1.29230	.19536	.03478	.00001	.13291	5.25765
TOTAL LOSS	37.91682	13.18241	116.15810	.25733	.04614	12.56607	540.38357

EFFICIENCY: .65

TABLE 4.4: The fundamental, harmonic losses and efficiency of the induction motor for slip = .02.

VARIABLE FREQUENCY POWER SUPPLY: CSI

HARMONIC ORDER	HARMONIC STEADY TORQUE
1	10.36132
5	-.00768
7	.00389
11	-.00079
13	.00056
17	-.00022
19	.00018
TOTAL TORQUE	10.35725

TABLE 4.5: Steady Harmonic Torque.

Produced in the Induction Motor for SLIP= .02

VARIABLE FREQUENCY POWER SUPPLY: CSI

HARM-ONIC ORDER	LOSS A	LOSS B	LOSS C	LOSS D	LOSS E	LOSS F	TOTAL LOSS HARMONIC
1	43.76443	5.17582	113.02144	.04454	.10150	19.19529	543.90906
5	1.75058	2.29261	.32003	.09996	.00023	2.40035	20.59129
7	.89315	2.07358	.29141	.07184	.00012	1.22327	13.66011
11	.36169	1.85045	.26344	.07862	.00004	.49562	9.14960
13	.25896	1.77810	.25638	.06675	.00003	.35455	8.14431
17	.15143	1.66243	.24692	.07225	.00002	.20720	7.02077
19	.12123	1.61215	.24370	.06478	.00001	.16573	6.62282
TOTAL LOSS	47.30147	16.44514	114.64332	.49874	.10195	24.04201	609.09796

EFFICIENCY: .71701

TABLE 4.6: The fundamental, harmonic losses and efficiency of the induction motor for slip = .03.

VARIABLE FREQUENCY POWER SUPPLY: CSI

HARMONIC ORDER	HARMONIC STEADY TORQUE
1	15.27513
5	-.00960
7	.00484
11	-.00099
13	.00070
17	-.00028
19	.00022
TOTAL TORQUE	15.27003

TABLE 4.7: Steady Harmonic Torque.

Produced in the Induction Motor for SLIP= .03

VARIABLE FREQUENCY POWER SUPPLY: CSI

HARM-ONIC ORDER	LOSS A	LOSS B	LOSS C	LOSS D	LOSS E	LOSS F	TOTAL LOSS HARMONIC
1	55.88818	6.60964	112.61967	.10503	.17950	33.94676	628.04636
5	2.23553	2.92772	.40883	.16924	.00039	3.06492	26.41989
7	1.14058	2.64801	.37224	.12193	.00020	1.56194	17.53468
11	.46189	2.36307	.33645	.13316	.00007	.63277	11.78223
13	.33070	2.27067	.32743	.11321	.00005	.45266	10.48413
17	.19338	2.12296	.31527	.12236	.00003	.26449	9.05551
19	.15481	2.05875	.31114	.10982	.00002	.21155	8.53829
TOTAL LOSS	60.40507	21.00082	114.69103	.87475	.18026	40.13509	711.86108

EFFICIENCY: .74585

TABLE 4.8: The fundamental, harmonic losses and efficiency of the induction motor for slip = .04.

VARIABLE FREQUENCY POWER SUPPLY: CSI

HARMONIC ORDER	HARMONIC STEADY TORQUE
1	20.26048
5	-.01228
7	.00617
11	-.00126
13	.00090
17	-.00035
19	.00028
TOTAL TORQUE	20.25394

TABLE 4.9: Steady Harmonic Torque.

Produced in the Induction Motor for SLIP= .04

VARIABLE FREQUENCY POWER SUPPLY: CSI

HARM-ONIC ORDER	LOSS A	LOSS B	LOSS C	LOSS D	LOSS E	LOSS F	TOTAL LOSS HARMONIC
1	71.42075	8.44661	112.96421	.20532	.28073	53.08987	739.22247
5	2.85683	3.74140	.52264	.26881	.00062	3.91625	33.91964
7	1.45757	3.38395	.47581	.19413	.00032	1.99579	22.52271
11	.59025	3.01982	.43000	.21157	.00011	.80845	15.18063
13	.42261	2.90174	.41845	.18012	.00008	.57832	13.50394
17	.24713	2.71298	.40282	.19441	.00004	.33787	11.68573
19	.19784	2.63092	.39752	.17464	.00004	.27023	11.01356
TOTAL LOSS	77.19298	26.83742	115.61145	1.42900	.28194	60.99678	847.04868

EFFICIENCY: .75800

TABLE 4.10: The fundamental, harmonic losses and efficiency of the induction motor for slip = .05.

VARIABLE FREQUENCY POWER SUPPLY: CSI

HARMONIC ORDER	HARMONIC STEADY TORQUE
1	25.34855
5	-.01571
7	.00788
11	-.00162
13	.00115
17	-.00045
19	.00036
TOTAL TORQUE	25.34015

TABLE 4.11: Steady Harmonic Torque.

Produced in the Induction Motor for SLIP= .05

VARIABLE FREQUENCY POWER SUPPLY: CSI

HARM-ONIC ORDER	LOSS A	LOSS B	LOSS C	LOSS D	LOSS E	LOSS F	TOTAL LOSS HARMONIC
1	90.32131	10.68189	.113.63819	.35597	.40559	76.70429	876.32172
5	3.61285	4.73151	.66117	.40561	.00094	4.95204	43.09240
7	1.84329	4.27947	.60189	.29364	.00048	2.52364	28.62722
11	.74646	3.81898	.54384	.31935	.00017	1.02217	19.35290
13	.53445	3.66965	.52921	.27226	.00012	.73118	17.21059
17	.31253	3.43093	.50930	.29343	.00007	.42711	14.92010
19	.25020	3.32716	.50258	.26384	.00005	.34160	14.05629
TOTAL LOSS	97.62109	33.93959	116.98618	2.20410	.40742	86.70203	1013.58122

EFFICIENCY: .761

TABLE 4.12: The fundamental, harmonic losses and efficiency of the induction motor for slip = .06.

VARIABLE FREQUENCY POWER SUPPLY: CSI

HARMONIC ORDER	HARMONIC STEADY TORQUE
1	30.51967
5	-.01990
7	.00994
11	-.00204
13	.00145
17	-.00057
19	.00045
TOTAL TORQUE	30.50899

TABLE 4.13: Steady Harmonic Torque.

Produced in the Induction Motor for SLIP= .06

VARIABLE FREQUENCY POWER SUPPLY: VSI

HARM-ONIC ORDER	LOSS A	LOSS B	LOSS C	LOSS D	LOSS E	LOSS F	TOTAL LOSS HARMONIC
1	30.66648	3.62678	122.126118	.00179	.01221	2.30905	476.22729
5	3.25076	4.25730	.59383	.06259	.00014	4.45850	37.86937
7	.85265	1.97956	.27803	.02301	.00004	1.16811	12.90422
11	.14296	.73142	.10410	.01047	.00001	.19599	3.55483
13	.07398	.50798	.07323	.00641	.00000	.10134	2.28883
17	.02591	.28447	.04226	.00417	.00000	.03549	1.17688
19	.01682	.22363	.03382	.00302	.00000	.02301	.90089
TOTAL LOSS	35.02956	11.61114	123.25145	.11146	.01240	8.29149	534.92231

EFFICIENCY: .48737

TABLE 4.14: The fundamental, harmonic losses and efficiency of the induction motor for slip = .01.

VARIABLE FREQUENCY POWER SUPPLY:·VSI

HARMONIC ORDER	HARMONIC STEADY TORQUE
1	5.51244
5	-.01777
7	.00464
11	-.00039
13	.00020
17	-.00005
19	.00003
TOTAL TORQUE	5.49911

TABLE 4.15: Steady Harmonic Torque.

Produced in the Induction Motor for SLIP= .01

VARIABLE FREQUENCY POWER SUPPLY: VSI

HARM-ONIC ORDER	LOSS A	LOSS B	LOSS C	LOSS D	LOSS E	LOSS F	TOTAL LOSS HARMONIC
1	36.76130	4.34759	120.35781	.01407	.04810	9.09590	511.87432
5	3.24993	4.25621	.59390	.12443	.00029	4.45679	38.04467
7	.85248	1.97916	.27806	.04587	.00008	1.16772	12.97006
11	.14292	.73118	.10408	.02082	.00001	.19588	3.58470
13	.07396	.50782	.07321	.01276	.00001	.10128	2.30711
17	.02590	.28434	.04224	.00828	.00000	.03545	1.18864
19	.01681	.22352	.03379	.00601	.00000	.02299	.90939
TOTAL LOSS	41.12330	12.32982	121.48309	.23224	.04849	15.07601	570.87889

EFFICIENCY: .65

TABLE 4.16: The fundamental, harmonic losses and efficiency of the induction motor for slip = .02.

VARIABLE FREQUENCY POWER SUPPLY: VSI

HARMONIC ORDER	HARMONIC STEADY TORQUE
1	10.85744
5	-.01779
7	.00463
11	-.00039
13	.00020
17	-.00005
19	.00003
TOTAL TORQUE	10.84407

TABLE 4.17: Steady Harmonic Torque.

Produced in the Induction Motor for SLIP= .02

VARIABLE FREQUENCY POWER SUPPLY: VSI

HARM-ONIC ORDER	LOSS A	LOSS B	LOSS C	LOSS D	LOSS E	LOSS F	TOTAL LOSS HARMONIC
1	45.88359	5.42643	118.49416	.04670	.10641	20.12477	570.24624
5	3.24912	4.25516	.59398	.18554	.00043	4.45512	38.21802
7	.85231	1.97877	.27808	.06856	.00011	1.16734	13.03550
11	.14287	.73097	.10406	.03106	.00002	.19578	3.61427
13	.07394	.50766	.07320	.01906	.00001	.10123	2.32526
17	.02589	.28421	.04221	.01235	.00000	.03542	1.20029
19	.01680	.22342	.03377	.00898	.00000	.02297	.91783
TOTAL LOSS	50.24452	13.40664	119.61946	.37225	.10698	26.10263	629.55741

EFFICIENCY: .72110

TABLE 4.18: The fundamental, harmonic losses and efficiency of the induction motor for slip = .03.

VARIABLE FREQUENCY POWER SUPPLY: VSI

HARMONIC ORDER	HARMONIC STEADY TORQUE
1	16.01478
5	-.01782
7	.00462
11	-.00039
13	.00020
17	-.00005
19	.00003
TOTAL TORQUE	16.00138

TABLE 4.19: Steady Harmonic Torque.

Produced in the Induction Motor for SLIP= .03

VARIABLE FREQUENCY POWER SUPPLY: VSI

HARMONIC ORDER	LOSS A	LOSS B	LOSS C	LOSS D	LOSS E	LOSS F	TOTAL LOSS HARMONIC
1	57.83831	6.84028	116.54935	.108577	.18577	35.13128	649.96099
5	3.24833	4.25413	.59405	.24591	.00057	4.45349	38.38943
7	.85215	1.97839	.27811	.09109	.00015	1.16696	13.10055
11	.14283	.73076	.10405	.04118	.00002	.19568	3.64355
13	.07391	.50751	.07318	.02530	.00001	.10117	2.34328
17	.02588	.28410	.04219	.01637	.00000	.03540	1.21183
19	.01679	.22333	.03375	.01191	.00000	.02295	.92620
TOTAL LOSS	62.19820	14.81850	117.67468	.540337	.18652	41.10693	709.57583

EFFICIENCY: .75302

TABLE 4.20: The fundamental, harmonic losses and efficiency of the induction motor for slip = .04.

VARIABLE FREQUENCY POWER SUPPLY: VSI

HARMONIC ORDER	HARMONIC STEADY TORQUE
1	20.96744
5	-.01784
7	.00461
11	-.00039
13	.00020
17	-.00005
19	.00003
TOTAL TORQUE	20.95400

TABLE 4.21: Steady Harmonic Torque.

Produced in the Induction Motor for SLIP= .04

VARIABLE FREQUENCY POWER SUPPLY: VSI

HARM-ONIC ORDER	LOSS A	LOSS B	LOSS C	LOSS D	LOSS E	LOSS F	TOTAL LOSS HARMONIC
1	72.41534	8.56424	114.53731	.20818	.28464	53.82919	749.51664
5	3.24757	4.25312	.59412	.30557	.00071	4.45189	38.55893
7	.85199	1.97802	.27813	.11347	.00019	1.16660	13.16520
11	.14280	.73056	.10403	.05118	.00003	.19558	3.67253
13	.07389	.50737	.07317	.03149	.00001	.10112	2.36118
17	.02587	.28399	.04217	.02035	.00000	.03537	1.22326
19	.01679	.22324	.03373	.014282	.00000	.02293	.93452
TOTAL LOSS	76.77425	16.54054	115.66266	.744522	.28558	59.80268	809.43226

EFFICIENCY: .76795

TABLE 4.22: The fundamental, harmonic losses and efficiency of the induction motor for slip = .05.

VARIABLE FREQUENCY POWER SUPPLY: VSI

HARMONIC ORDER	HARMONIC STEADY TORQUE
1	25.70154
5	-.01786
7	.00460
11	-.00039
13	.00020
17	-.00005
19	.00003
TOTAL TORQUE	25.688

TABLE 4.23: Steady Harmonic Torque.

Produced in the Induction Motor for SLIP= .05

VARIABLE FREQUENCY POWER SUPPLY: VSI

HARM-ONIC ORDER	LOSS A	LOSS B	LOSS C	LOSS D	LOSS E	LOSS F	TOTAL LOSS HARMONIC
1	89.39414	10.57224	112.47167	.35231	.40143	75.91690	867.32609
5	3.24682	4.25214	.59419	.36452	.00085	4.45033	38.72654
7	.85184	1.97767	.27815	.13570	.00022	1.16625	13.22947
11	.14276	.73038	.10401	.06108	.00003	.19549	3.70123
13	.07387	.50724	.07315	.0373	.00002	.10107	2.37895
17	.02586	.28390	.04214	.02428	.00001	.03534	1.23458
19	.01678	.22316	.03371	.01770	.00000	.02291	.94277
TOTAL LOSS	93.75207	17.84673	113.59702	.99322	.40256	81.88829	927.53963

EFFICIENCY: .77358

TABLE 4.24: The fundamental, harmonic losses and efficiency of the induction motor for slip = .06.

VARIABLE FREQUENCY POWER SUPPLY: VSI

HARMONIC ORDER	HARMONIC STEADY TORQUE
1	30.20638
5	-.01789
7	.00459
11	-.00039
13	.00020
17	-.00005
19	.00003
TOTAL TORQUE	30.19288

TABLE 4.25: Steady Harmonic Torque.

Produced in the Induction Motor for SLIP= .06

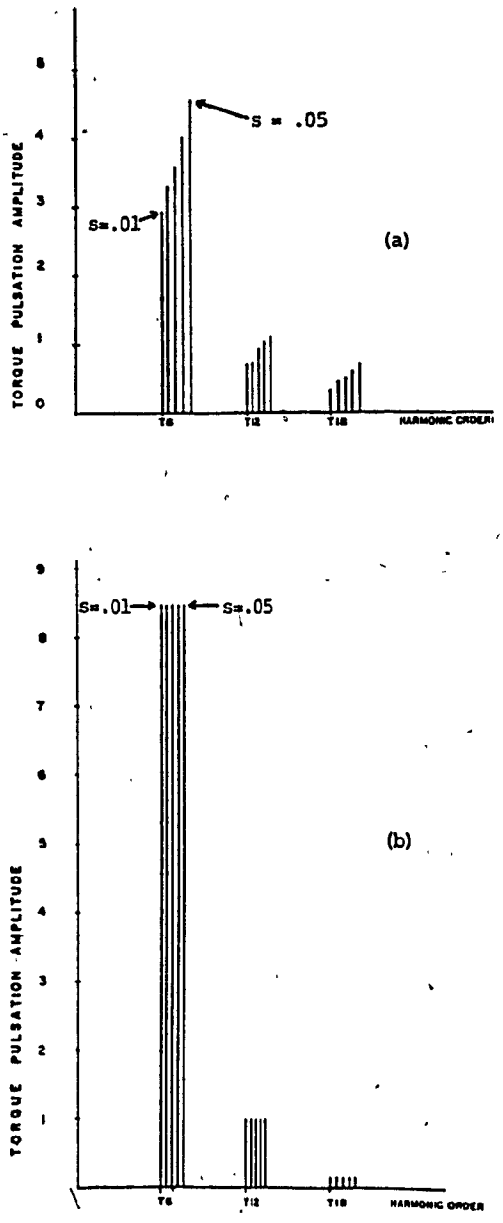

FIG.4.3 SPECTRA OF PULSATING TORQUES (A)VSI (B)CSI FOR DIFFERENT VALUES OF SLIP.

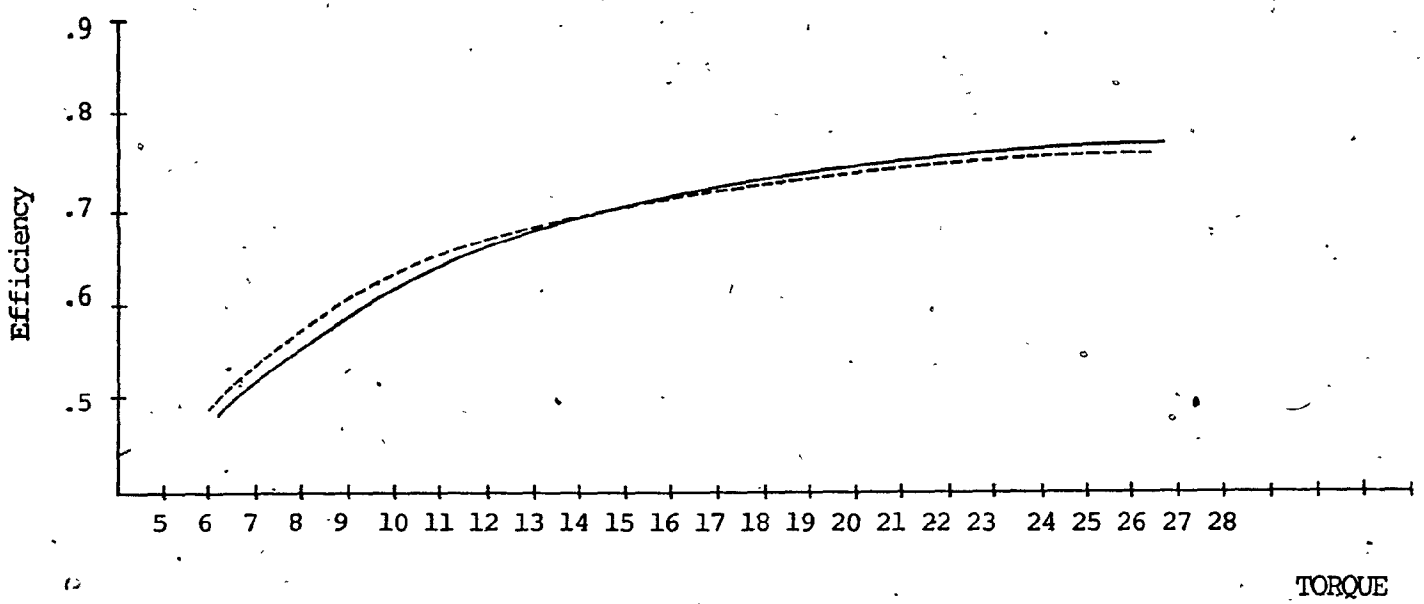

FIG. 4.4 THE GRAPH OF EFFICIENCY VS TORQUE.

———— VSI

- - - - - - - CSI

CHAPTER 5

CONCLUSION

This thesis has shown a systematic method of comparing the losses in a squirrel cage induction motor when fed by VSI and CSI as part of a variable speed drive. The compelling reason for the increased interest in this field lies in the fact that the squirrel cage induction motor is the one which is extensively used in industry. In addition, the energy crisis has amplified this interest due to the increased efficiency of inverters using thyristors for control. The comparison study is the best way to find out whether voltage source or current source inverter better suits the squirrel cage induction motor for a particular application.

The method which was followed in this thesis, was to decompose a dc link ac drive into its basic components. Then it analysed them separately. The various losses occuring in each part were classified and their locations were determined. Finally the mathematical expressions were provided in order to calculate the losses. It was however impossible to provide general mathematical expression for the losses occuring in the commutation circuits. This is due to the fact that Commutation Circuits vary from design to design. The advantage of this method is twofold. First, it helps the design engineer to size properly the systems and to size protection devices such as heat sink, etc. Second, it helps application engineer to choose the most efficient system. Among other factors, the power factor and torque pulsations were also computed to give more information about these two systems.

Chapter four demonstrated the characteristics of a six-step square wave voltage source inverter and its dual, the six-step square wave current source inverter. Then output voltage and current wave forms were computed and compared. Their power factors were also compared. The load losses occuring in the rectifier and inverter components were compared in each system.

The time fundamental and harmonic losses occuring in the induction motor stator and rotor from both power supplies were calculated and compared. Finally figure 4.4 demonstrated that when a standard induction motor is fed by a six-step current and voltage power supplies it has the same efficiency at rated torque. For the output torque greater than rated torque, the voltage source inverter is more efficient, whereas for the output torque less than rated torque the current source is more efficient. It should be emphasized that the air gap flux was kept constant in both systems.

The torque pulsations produced by the different power supplies were also compared, fig. 4.3. It is evident from fig. 4.3 that the sixth harmonic torque is the most significant one in both systems. In the case of the CSI-fed motor, the magnitudes of the pulsating torque components are independant of slip whereas those of the VSI-fed motor increase with increasing slip.

It is hoped the method which was used in this thesis may be considered as a guideline for future studies.

REFERENCES

(1) Mohamad Abbas, D.W. Novotny, "Stator Referred Circuits for Inverter Driven Electric Machines", IEEE-IAS-1978, PP 828-835, Annual Meeting.

(2) Douglas Schaley, "Induction Motor for Variable Frequency Power Supplies", IEEE Trans-IA, Vol. IA-18, No. 4, July, August 1982.

(3) Andrew J. Humphrey, "Inverter Commutation Circuits", IEEE Trans-IA, Vol. IGA-4, PP 104-110, Jan/Feb. 1968.

(4) W. McMurray, "Optimum Snubbers for Power Semiconductors", Trans. IEEE IA 72, Sept/Oct., PP 593-600.

(5) P. DeBruyne and H. Lawatseh, "Blocking Voltage Characteristics During Turn-off of a Semiconductor Power Device in RC Connection", Brown Boverie Rev. No. 5, 1975, PP 220-224.

(6) J.B. Rice and L.E. Nichels, "Commutation $dv/_{dt}$ Effects in Thyristor Three-Phase Bridge Converters", IEEE Trans. IGA, Nov./Dec. 1968, PP 665-672.

(7) T.H. Barton, "Snubber Circuits for Thyristor Converter", Conference Record, IEEE-IA-1978, PP 1086-1092, Annual Meeting.

(8) B.J. Chalmers, B.R. Sarkar, "Induction Motor Losses due to Nonsinusoidal Supply Waveforms", Proc. IEEE, Vol. 115, No. 12, Dec. 1968.

(9) Alger, P.L., Angst, G. and Davies, E.J., "Stray Losses in Polyphase Induction Machines", AIEE Trans (PAS), Vol. 78. Pt. III-A, June 1959, PP 349-357.

(10) K. Venkatesan, J.F. Lindsay, "Comparative Study of the Losses in Voltage and Current Source Inverter fed Induction Motors.", IEEE Transactions on IA, Vol. IA - 18, No. 3, May/June 1982.

(11) Stuart D.T. Robertson, K.M. Hebbon, "Torque Pulsations in Induction Motors with Inverter Drives", IEEE Trans., Ind. Gen. Appl. Vol. IGA-7, PP 318-323, Mar/Apr. 1971

(12) John M.D. Murphy, "Thyristor Control of AC Motors", Pergamon Press Ltd., 1973.